**The Thesis Committee for Zeyu Yan**
**Certifies that this is the approved version of the following thesis:**

# Optimal Control for A Modern Wind Turbine System

**APPROVED BY**
**SUPERVISING COMMITTEE:**

**Supervisor:**

Dongmei Chen

David G. Hull

# Optimal Control for A Modern Wind Turbine System

**by**

**Zeyu Yan, B. E**

**Thesis**

Presented to the Faculty of the Graduate School of

The University of Texas at Austin

in Partial Fulfillment

of the Requirements

for the Degree of

**Master of Science in Engineering**

**The University of Texas at Austin**

**May 2012**

## Acknowledgements

First of all, I would like to thank my dear advisor, Professor Dongmei Chen. She gave me a lot of help on my research and career plan. She is always ready to help me when I met problems, no matter how busy she is. She is such a nice person and nothing is able to express my gratitude to her at this time.

Second, I would like to thank Professor David Hull for teaching me the numerical methods of optimal control and helping me revising my thesis. I really enjoy Professor Hull's class and I learned a lot from him. When he was very busy at the end of the semester, he is still eager to help me revise my thesis. No words are able to show my gratitude to him.

Third, I would like to thank my dear friend, Garrett Anderson for his help on revising my thesis. He was very busy and tired doing his job when I sent my thesis to him. He didn't complain and helped me on the revising with a high efficiency. I just want to tell him that I will treat you for a big meal next time we meet each other.

Finally, I would like to thank my girl friend Meggie Yuan, my roommate Yunping Fei and all of my friends. I would not be able to finish all of the tasks without your support. Thank you very much!

# Abstract

## Optimal Control for A Modern Wind Turbine System

Zeyu Yan, M. S. E

The University of Texas at Austin, 2012

Supervisor: Dongmei Chen

Wind energy is the most abundant resource in the renewable energy portfolio. Increasing the wind capture capability improves the economic viability of this technology, and makes it more competitive with traditional fossil-fuel based supplies. Therefore, it is necessary to explore control strategies that maximize aerodynamic efficiency, thus, the wind energy capture.

Several control algorithms are developed and compared during this research. A traditional feedback control is adapted as the benchmark approach, where the turbine torque and the blade pitch angle are used to control the wind turbine operation during partial and full load operations, correspondingly. Augmented feedback control algorithms are then developed to improve the wind energy harvesting. Optimal control methodologies are extensively explored to achieve maximal wind energy capture. Numerical optimization techniques, such as direct shooting optimization are employed. The direct shooting method convert the optimal control problem into a parameter optimization problem and use nonlinear programming algorithm to find the optimal

solution. The dynamic programming, a global optimization approach over a time horizon, is also investigated. The dynamic programming finds the control inputs for the blade pitch angle and speed ratio to maximize the power coefficient, based on historical wind data.

A dynamic wind turbine model has been developed to facilitate this process by characterizing the performance of the various possible input scenarios. Simulation results of each algorithm on real wind site data are presented to compare the wind energy capture under the proposed control algorithms with the traditional feedback control design. The result of the tradeoff analysis between the computation expense and the energy capture is also reported.

# Table of Contents

# List of Tables

# List of Figures

# Chapter 1: *Introduction*

## BACKGROUND

Wind energy, considered as one of the renewable resources, is becoming more important in displacement of the fossil fuel to provide electric energy. It is a widely distributed and plentiful resource. The total amount of economically extractable power available from the wind is considerably more than present human power use from all other sources [1]. Besides, the wind energy is clean and won't generate greenhouse effect. Therefore, utilization of wind energy has rapidly increased in recent years. Although wind is still not the main energy source for the utility grid, the penetration of wind energy has increased by 4 times from 1999 to 2005. By the year of 2008, the electrical power generated from the wind is 94.1 million kW all over the world.

As an important device that converts the kinetic energy from the wind into mechanical energy, maximizing the efficiency of wind turbine plays an important role in the development of the wind power. Especially in s wind farm where hundreds of wind turbines are installed, the efficiency improvement of an individual wind turbine could result in a significant energy gain for the entire wind farm. This will make the wind energy more economically viable.

A well-designed real-time controller plays a key role in maximizing the wind energy capture. Various control methods are developed to realize different purposes. Some of the methods aim to maximize the total wind energy capture and some aim to

generate a higher generator input torque. There are also other types of methods, which can be used to regulate turbine speed for safety requirements.

## WIND TURBINE OPERATION

Different regions are defined in which the turbines operate. In Region 1, the wind speed is too low to warrant turbine startup. The blades are pitched at full feather. Once the wind speed is large enough for machine start-up, the blades are pitched to the normal Region 2 angle. In Region 2, the wind speed and the generator torque are below "rated." Blade pitch is held constant at the optimal value that gives the maximum aerodynamic torque. In Region 2.5, the wind speeds are approaching those that provide rated power. This is a transition region where the torque command is commonly computed as an affine function of generator speed such that rated torque is reached before the rated generator speed. In Region3, the wind speed is at or above that which will generate rated power. The generator torque is held constant at rated, and blade-pitch control is used to limit aerodynamic power by regulating turbine speed at the rated speed.

## REVIEW OF TURBINE CONTROL METHODS

In Jason H. Laks, Lucy Y. Pao, and Alan D. Wright's paper [2-5], a feedback control method is mentioned, which is mainly used for Region 2 control of turbine systems. In this feedback control method, the generator input torque is obtained as a function of rotor speed, which will drive the system to reach the point of maximum wind power capture. While using this feedback law, the turbine is treated as a single input, single output (SISO) system. This method can be easily applied with satisfying performance. Details of this feedback method will be discussed in Chapter 4.

In the same paper, a classical proportional-integral-derivative (PID) control technique is introduced for the design of the blade pitch controller. This PID control method is used in Region 3 to regulate turbine speed in the presence of varying wind conditions. Further discussions on methods for choosing the gains are found in [6]. It is also revealed that the standard PID control can be augmented with notch transfer functions to add damping to known resonances.

In addition, advanced control methods are also discussed in [2-5]. In Region 2, research is further divided between investigations that incorporate detailed models of the generator electromechanical system and power electronics and those that view the generator torque in terms of a static gain that responds instantly to commanded torque. Where studies involve electromechanical models, advanced research congregates around maximum power point tracking (MPPT) and sliding mode approaches [7-8] or extremum seeking control. On the other hand, time invariant, multiple inputs, multiple outputs (MIMO) methods [9-10] tend to be the most prevalent in the research of advanced controls or Region 3, but adaptive [11-14] and novel gain-scheduling [15] approaches are also investigated.

A small number of papers have been published regarding adaptive control of wind turbines [11-14], but most involve Region 3 control, and very few attempts have been made to test these advanced controls on real turbines. The control law is defined separately for positive and negative regions of the rotor speed because it is undesirable to apply torque control when the turbine is spinning in reverse. The simulation of this adaptive method shows that the adaptation behavior with the longer adaption period is

significantly better than the behavior with the shorter adaption period. Stability analysis is also used for the adaptive control to prove the convergence.

# Chapter 2: *Wind turbine modeling*

## TURBINE STRUCTURE

Figure 1 [16] shows the structure of a modern wind turbine system and main components are numbered. The rotor is the component, which, with the help of the blades, converts the energy in the wind into rotary mechanical movement. The pitch refers to turning the angle of attack of the blades into or out of the wind. The gearbox converts the rotor motion into the approximate range, which the generator requires. The generator is the component, which converts mechanical movement into electrical energy.

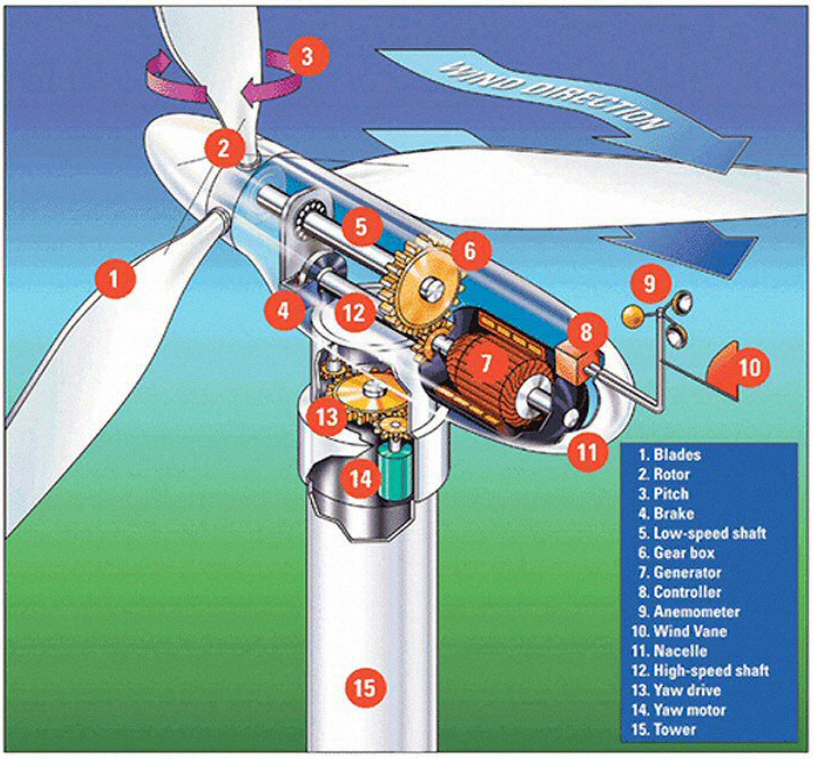


Figure 1: Turbine structure

**SYSTEM CONSTRAINTS**

The following physical constraints must be satisfied for the controller design:

$$\begin{aligned} \omega_{rotor_{\min}} \le \omega_{rotor} \le \omega_{rotor_{\max}} \\ \beta_{rotor_{\min}} \le \beta_{rotor} \le \beta_{rotor_{\max}} \\ \dot{\beta}_{rotor_{\min}} \le \dot{\beta}_{rotor} \le \dot{\beta}_{rotor_{\max}} \\ 0 < \tau_{generator} \le \tau_{\max} \end{aligned} \tag{1}$$

All of the control inputs and states must have certain upper and lower limits. Sometimes the pitch angle acceleration has also been limited to imitate normal operating capability.

All these parameters of the wind turbine system used in this simulation are also given in Table 1. Before discussing various control strategies of a modern system, the system equations of motion need to be derived first.

| Parameter | Value |
|---|---|
| Rotor moment of inertia, $J$ | $1.5 \times 10^4 \ \ kg \cdot m^2$ |
| Rotor diameter, $\boldsymbol{D_r}$ | 18.50 $m$ |
| Gear ratio, $\boldsymbol{G_r}$ | 21.5858 |
| Maximum generator angular velocity, $\boldsymbol{\omega_{max}}$ | 1800 $RPM$ ×70% |
| Minimum generator angular velocity, $\boldsymbol{\omega_{min}}$ | 1800 $RPM$ × 130% |
| Maximum rotor pitch angle, $\boldsymbol{\beta_{max}}$ | 15° |
| Minimum rotor pitch angle, $\boldsymbol{\beta_{min}}$ | 0° |
| Maximum generator input torque, $\boldsymbol{\tau_{max}}$ | 3000 $N \cdot m$ |

Table 1: Turbine system parameters

**TURBINE DYNAMICS**

The model is developed evaluate the performance of the input parameters. For the control study the drivetrain assembly is assumed to be rigid and have no energy loss. The dynamics of the wind turbine can be represented by:

$$\dot{\omega} = \frac{1}{J}(\tau_{aero} - \tau_c) \tag{2}$$

where $J$ is the combined rotational inertia of the rotor, gearbox, generator and shafts, $\tau_{aero}$ is the aerodynamic torque, which drives the wind turbine, and $\tau_c$ is the reactive torque feedback. The aerodynamic torque is defined as:

$$\tau_{aero} = \frac{P}{\omega} \tag{3}$$

where $P$ is the aerodynamic rotor power and $\omega$ is the turbine rotor speed. The relation between the aerodynamic rotor power $P$ and the available wind power $P_{wind}$ are defined by the power coefficient $C_p$. This measures how effectively the wind can be converted to mechanical energy and is defined as:

$$C_p = \frac{P}{P_{wind}} \tag{4}$$

The available wind power $P_{wind}$ is calculated using Equation (5):

$$P_{wind} = \frac{1}{2}\rho_{air} A V_w^3 \tag{5}$$

where $\rho_{air}$ is the density of air, and $V_w$ is the input wind speed. $A$ is the rotor swept area, which is defined by:

$$A = \pi R_r^2 = \frac{1}{4}\pi D_r^2 \tag{6}$$

where $R_r$ is the turbine rotor radius and $D_r$ is the rotor diameter.

The reactive torque feedback $\tau_c$ in Equation (1) is defined in Equation (7):

$$\tau_c = \tau G_r \tag{7}$$

where $\tau$ is the generator input torque and $G_r$ is the gearbox gear ratio defined as the generator shaft speed over the rotor shaft speed.

By combining all of equations above, the dynamic model of the integrated system can be represented by:

$$\dot{\omega} = \frac{1}{J}(\frac{\pi}{8} D_r^2 \rho_{air} C_p \frac{V_w^3}{\omega} - \tau G_r) \tag{8}$$

The power coefficient $C_p$ is a non-linear function of the blade pitch angle $\beta$ and the tip speed ratio $\lambda$:

$$C_p = f(\lambda, \beta) \tag{9}$$

The tip speed ratio $\lambda$ is defined as the linear velocity of the rotor over wind speed and is shown as follows:

$$\lambda = \frac{\omega D_r}{2V_w} \tag{10}$$

From Equation (8), it is seen that a modern wind turbine system is a multiple input, single output (MISO) system. The two control inputs are the rotor pitch angle and the generator input torque. The single output is the rotor angular velocity.

**AERODYNAMIC COEFFICIENT $C_p$**

The aerodynamic coefficient $C_p$ is a nonlinear function of the blade pitch angle and the tip speed ratio. A formula has been developed by Heier [23] is used to approximate the power coefficient and is shown in Equations (11) and (12):

$$C_p = c_1(\frac{c_2}{\lambda_i} - c_3\beta - c_4\beta^x - c_5)e^{-\frac{c_6}{\lambda_i}} \tag{11}$$

where,

$$\frac{1}{\lambda_i} = \frac{1}{\lambda + 0.08\beta} - \frac{1}{\beta^3 + 1} \tag{12}$$

All of the c's and x are constants.

The surface plot, shown in Figure 2, illustrates how the power coefficient $C_p$,varies with changes in the rotor pitch angle, $\beta$ and the speed ratio, $\lambda$. The power coefficient $C_p$ is an important measurement of how much wind energy is captured by the turbine system. When time is held constant, maximizing energy capture is equivalent to maximize the turbine power. Since the amount of available wind energy is also fixed, maximize wind power capture is the same as maximize the power coefficient, $C_p$. This can be seen in Equation (4). The theories behind all control strategies, which aim to maximize wind energy capture is to find the best combinations of $\lambda$ and $\beta$, which maximize $C_p$ as wind speed varies.

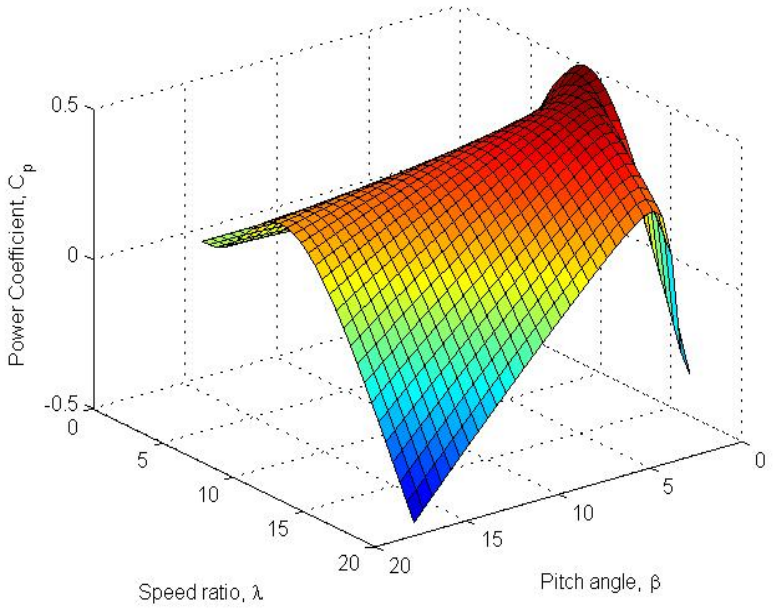


Figure 2: Surface plot of $C_p$ vs. $\lambda$ and $\beta$.

A plot of $C_p$ versus $\lambda$ under different $\beta$ values is also given in Figure 3. This figure shows how different combinations of $\lambda$ and $\beta$ can produce local maximum for the power coefficient. In Figure 3, $\beta$ ranges from 0° to 25°. The plot shows that a pitch angle of 25° will produce a maximum power coefficient at low values of $\lambda$. For a 0°, maximum performance is achieved when the speed ratio is around 7. For pitch angles 1° or 2°, peak performance shifts even more to the right. This is because when the rotor angular velocity or wind speed input changes, the location of $\lambda$ on the horizontal axis will change also. At this point the task is to find the corresponding $\beta$ that matches the speed coefficient that will generate the optimal $C_p$ value that will maximize wind energy capture. Table 2 shows the constant values of c's and x, which we use to generate the $C_p$ surface:

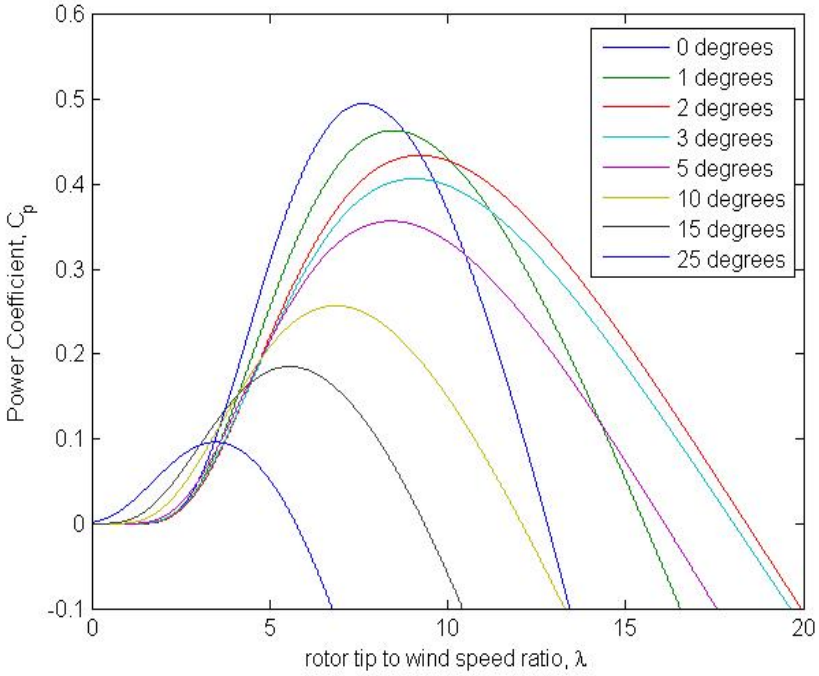


Figure 3: Plot of $C_p$ vs. $\lambda$.

| Name | $c_1$ | $c_2$ | $c_3$ | $c_4$ | $c_5$ | $c_6$ | x |
|---|---|---|---|---|---|---|---|
| Value | 0.5 | 116 | 0.4 | 5 | 19 | 0.08 | 3 |

Table 2: Values of c's and x.

# Chapter 3: *Wind speed profile*

This chapter talks about the selection of the wind speed profile for the simulation and how to classify wind data.

## WIND POWER CLASSES

The wind speed profile was obtained from the NREL official website [24]. The frequency of the wind speed data is every ten minutes. This frequency is too low and does not represent the real wind speed that often varies much faster. The assumption was made that the wind speed will keep a constant value within every one minute. A power spectral density function approach [25] is then used here to convert the frequency of the wind speed to every one minute.

Wind power classes are classified by their wind power density and speed. Table 2 [26] shows the different classes of wind power density at 10m and 50m.

| Wind Power Class* | 10 m (33 ft) | | 50 m (164 ft) | |
|---|---|---|---|---|
| | Wind Power Density (W/m2) | Speed m/s (mph) | Wind Power Density (W/m2) | Speed m/s (mph) |
| 1 | 0 | 0 | 0 | 0 |
| 2 | 100 | 4.4 (9.8) | 200 | 5.6 (12.5) |
| 3 | 150 | 5.1 (11.5) | 300 | 6.4 (14.3) |
| 4 | 200 | 5.6 (12.5) | 400 | 7.0 (15.7) |
| 5 | 250 | 6.0 (13.4) | 500 | 7.5 (16.8) |
| 6 | 300 | 6.4 (14.3) | 600 | 8.0 (17.9) |
| 7 | 400 | 7.0 (15.7) | 800 | 8.8 (19.7) |
| | 1000 | 9.4 (21.1) | 2000 | 11.9 (26.6) |

Table 3: Classes of wind power density at 10m and 50m.

# Chapter 4: *Feedback control design*

## TRADITIONAL METHOD

For traditional feedback control [2-5], the blade pitch is held constant at the optimal value $\beta_*$ that gives maximum wind energy capture. The turbine rotor velocity is controlled according to a feedback law shown in Equation (15):

The generator torque is set as:

$$\tau_c = K\hat{\omega}^2 \tag{13}$$

$\hat{\omega}$ is the measurement of the rotor speed and $K$ is has the form of:

$$K = \frac{1}{2}\rho_{air}\pi R^5 \frac{C_{p_{\max}}}{\lambda_*^3} \tag{14}$$

$C_{p_{max}}$ is the maximum power coefficient that the system can achieve, and $\lambda_*$ is the corresponding speed ratio.

Assume $\hat{\omega} = \omega$ (perfect measurements), and by combining Equation (8), Equation (15) is found:

$$\dot{\omega} = \frac{1}{2J}\rho_{air}R^5\omega^2\left(\frac{C_p}{\lambda^3} - \frac{C_{p_{\max}}}{\lambda_*^3}\right) \tag{15}$$

and

$$\begin{cases} \dot{\omega} < 0 \ \ when \ \ C_p < \dfrac{C_{p_{max}}}{\lambda_*^3}\lambda^3 \\ \dot{\omega} > 0 \ \ when \ \ C_p > \dfrac{C_{p_{max}}}{\lambda_*^3}\lambda^3 \end{cases}$$

It can be seen that this control law causes the turbine to accelerate toward the desired set point when the rotor speed is too slow and decelerate when the rotor speed is too fast.

**FIRST MODIFICATION**

The traditional feedback control is an unconstrained method that doesn't consider the system constraints. For most of the cases, the controls and the states have their certain ranges. Therefore, some modifications need to be developed for the traditional feedback control strategy.

The first modification is to limit the turbine rotor angular velocity. A logic controller was also developed, which controls the reactive torque feedback $\tau_c$ depending on several different cases to make sure that the rotor is running within the acceptable speed range.

$$\tau_c = \begin{cases} \tau_{aero}, \ if \ \ \dot{\omega} \geq 0 \ \ and \ \ \omega \geq \omega_{\max}; \\ \tau_{aero}, \ if \ \ \dot{\omega} \leq 0 \ \ and \ \ \omega \leq \omega_{\min}; \\ K\hat{\omega}^2, \ if \ \ \omega_{\min} \leq \omega \leq \omega_{\max}; \\ K\hat{\omega}^2, \ if \ \ \dot{\omega} \leq 0 \ \ and \ \ \omega \geq \omega_{\max}; \\ K\hat{\omega}^2, \ if \ \ \dot{\omega} \geq 0 \ \ and \ \ \omega \leq \omega_{\min}; \end{cases}$$

**SIMULATION RESULTS I**

The modified feedback control was applied to three different wind profiles by simulating the performance of each through 24 hours of site wind data. The wind speed data was unique in each case, representing three categories of wind, power classes 5 through 7, which are defined in Table 3. Most of the current wind farms are located at sites with wind class 5 and higher. Figure 4 shows the plots of wind speed profile versus time.

For all 3 simulations, modified feedback control method developed through Equations (13) to (15) is applied. $C_{p_{max}}$ is the global maximum and $\lambda_*$ is the corresponding speed ratio. Since the global maximum value of $C_p$ is achieved when the pitch angle $\beta$ is 0°, $\beta$ is held constant at 0° during the simulations.

Figure 5 shows the plot of the power coefficient $C_p$ versus time. From the plot, one can see that when the global maximum of $C_p$ is reachable, or the local maximum value is close to the global maximum, this modified feedback control strategy performs well and the global maximum is reached. When the global maximum is not reachable, the performance degrades. One can see that in Figure 5, there is a time interval in which the $C_p$ value is relative low for a class 5 wind speed input.

Figure 6 shows the plot of the rotor angular velocity versus time. From the plot, one can see that after the logic controller is added, the rotor angular velocity will be within the proper range.

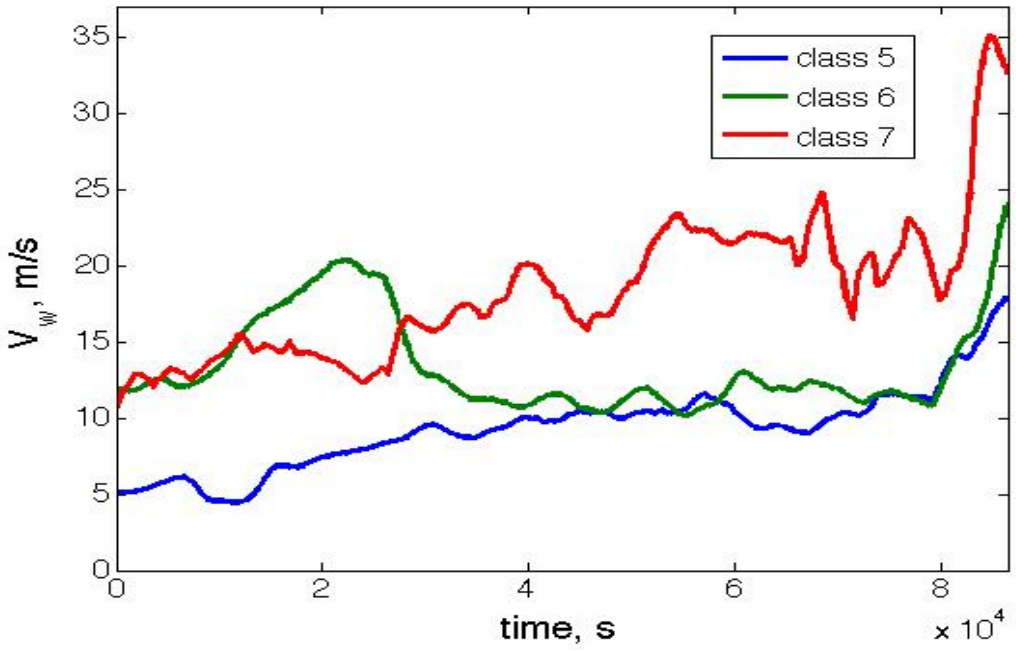


Figure 4: Plot of wind speed inputs from different wind power classes vs. time.

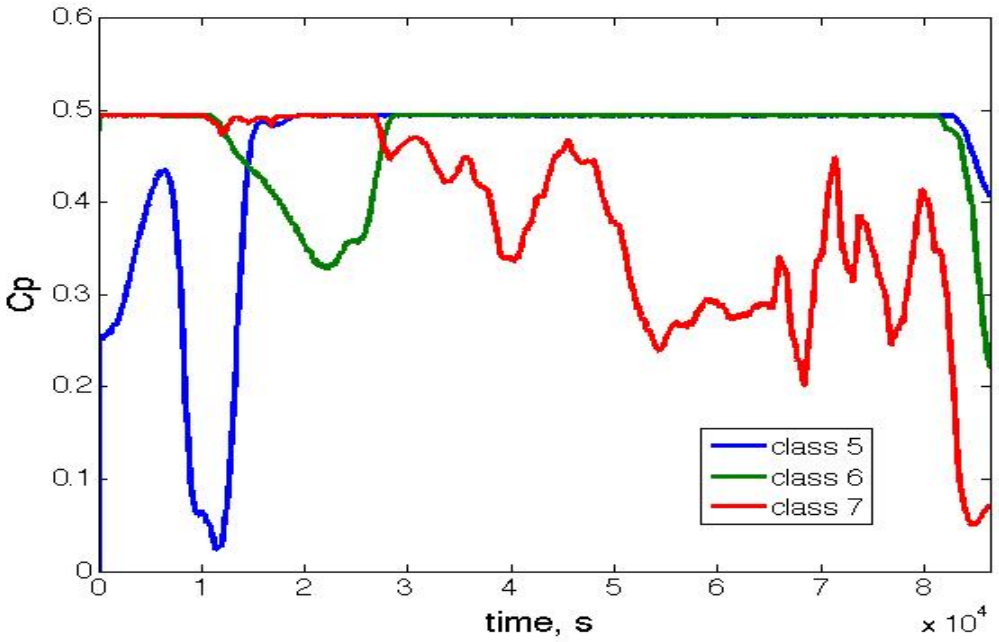


Figure 5: Plot of power coefficient vs. time using the first version of the feedback method.

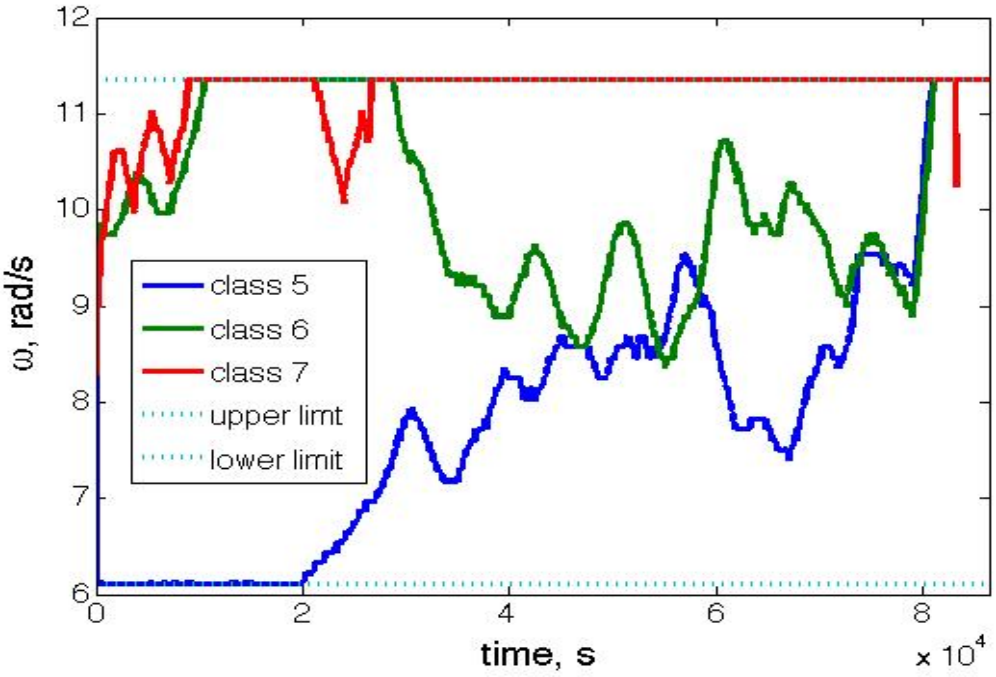


Figure 6: Plot of rotor angular velocity vs. time using the first version of the feedback control method.

**SECOND MODIFICATION**

For the traditional feedback control, since there are no constraints, the global maximum value of $C_p$ is always reachable, which makes the control strategy very efficient. The term $\frac{C_{pmax}}{\lambda_*^3}$ in Equations (14) and (15) will have a constant value, which is:

$$\frac{C_{p_{\max}}}{\lambda_*^3} = \frac{(C_{p_{\max}})_{global}}{(\lambda_*^3)_{global}} \tag{16}$$

where $(C_{p_{max}})_{global}$ and $(\lambda_*)_{global}$ are both constants.

However, due to the constraints on $\lambda$, the range of the rotor angular velocity is limited. According to Equation (10), the range of $\lambda$ will also vary with wind speed. When $\lambda$ is constrained to fall into an interval, which does not include $(\lambda_*)_{global}$, the global maximum value of $C_p$, $(C_{p_{max}})_{global}$ is no longer reachable. In this case, different combinations of the speed ratio, $\lambda$ and pitch angle, $\beta$ will generate different local maximum values of $C_p$.

$$\frac{C_{p_{\max}}}{\lambda_*^3} = \frac{(C_{p_{\max}})_{local}}{(\lambda_*^3)_{local}} \tag{17}$$

Because of this issue, a predictive algorithm must be applied to calculate the local maximum value of $C_p$. The corresponding $\lambda$ and $\beta$ values must also be found every time wind speed changes. The problem can be formulated as follows:

Find $(\lambda_*)_{local}$ and $(\beta_*)_{local}$, which maximize:

$$J = C_p(\lambda, \beta)$$

subjected to:

$$\omega_{\min} \le \omega \le \omega_{\max}$$
$$\beta_{\min} \le \beta \le \beta_{\max}$$

This constrained optimization problem can be solved by using a nonlinear programming algorithm or the 'fmincon' function in the *MATLAB* optimization toolbox.

After $(\lambda_*)_{local}$ and $(\beta_*)_{local}$ are found, the next step is to use the feedback control strategy to make $\lambda$ and $\beta$ reach these values quickly. Since the change of the pitch angle can be directly controlled, to reach $(\beta_*)_{local}$ as quickly as possible, a piecewise function will be used:

$$\begin{cases} \dot{\beta} = \dot{\beta}_{max} \ \ if \ \ \beta < (\beta_*)_{local} \\ \dot{\beta} = \dot{\beta}_{min} \ \ if \ \ \beta > (\beta_*)_{local} \end{cases}$$

The feedback control of the rotor angular velocity can be realized by Equation (15), the only difference is that the term $\frac{C_{p_{max}}}{\lambda_*^3}$ is replaced by $\frac{(C_{p_{\max}})_{local}}{(\lambda_*^3)_{local}}$. In this way, the second constrained modification on the traditional feedback control can be well applied.

The disadvantage of this modified feedback control method is that constraints on the generator input torque are still difficult to apply. Using this control strategy, the generator input torque is always positive, but there is no guaranty the upper limit of the constraint could be satisfied. In addition, the potential for further efficiency increase is not clear. An optimal control algorithm that enables the maximum wind energy capture is desirable.

**SIMULATION RESULTS II**

Figure 7 shows the plot of the power coefficient $C_p$ versus time and one can see that the $C_p$ curve generated by this control strategy always reaches local maximum values as expected when the wind speed changes. When the global maximum value is

reachable, the local maximum is the same as global maximum. The global maximum value is almost 0.5 in Figure 7.

Figure 8 shows the plot of the turbine angular velocity versus time. One can see that when the predictive controller is added, the turbine rotor angular velocity will always be within the proper range and never exceed its limits.

Figure 9 shows the plot of the rotor pitch angle versus time. It is seen that there are frequently changes of $\beta$ for wind speed input of class 5 at the beginning of the simulation. During this period, different pitch angles give different local maximum values of $C_p$. Even for constant $\beta$ values, the local maximum of $C_p$ may still differ.

Figure 10 shows the plot of the generator input torque versus time. The generator torque is always positive, which means that the generator doesn't perform like a motor. However, as mentioned above, there is no upper limit for the generator input torque. From Figure 10, we can see that as wind speed increases, the generator input torque can exceed 2500 $N*m$. Although one may expect the generator input torque to be as large as possible, there should be certain hardware constraints, which prevent the system from damaging. One way to solve this problem is to use some energy-storing device like batteries to store the extra energy.

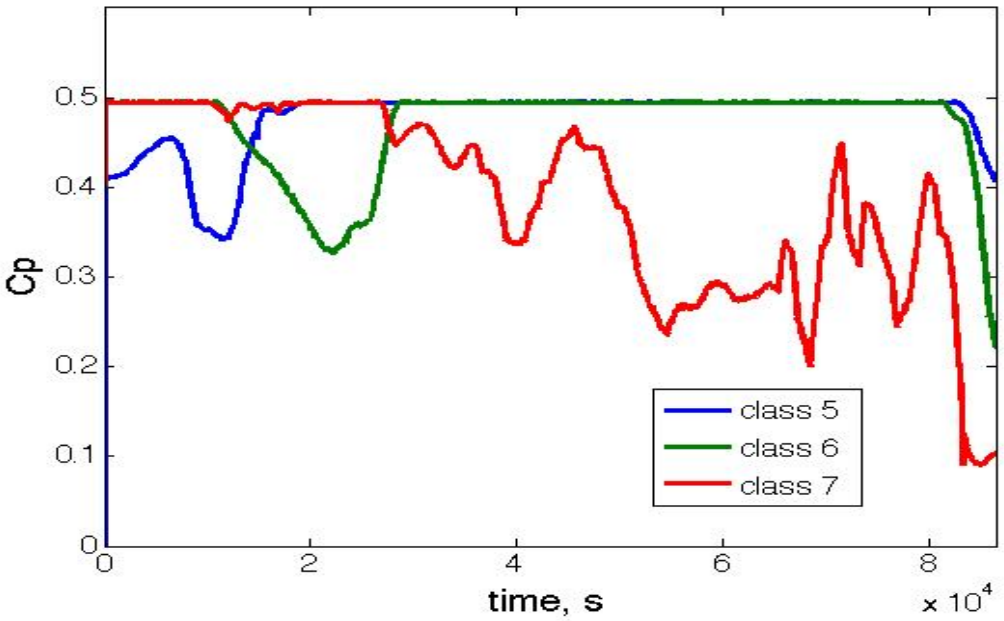


Figure 7: Plot of power coefficient vs. time using the second version of the feedback control method.

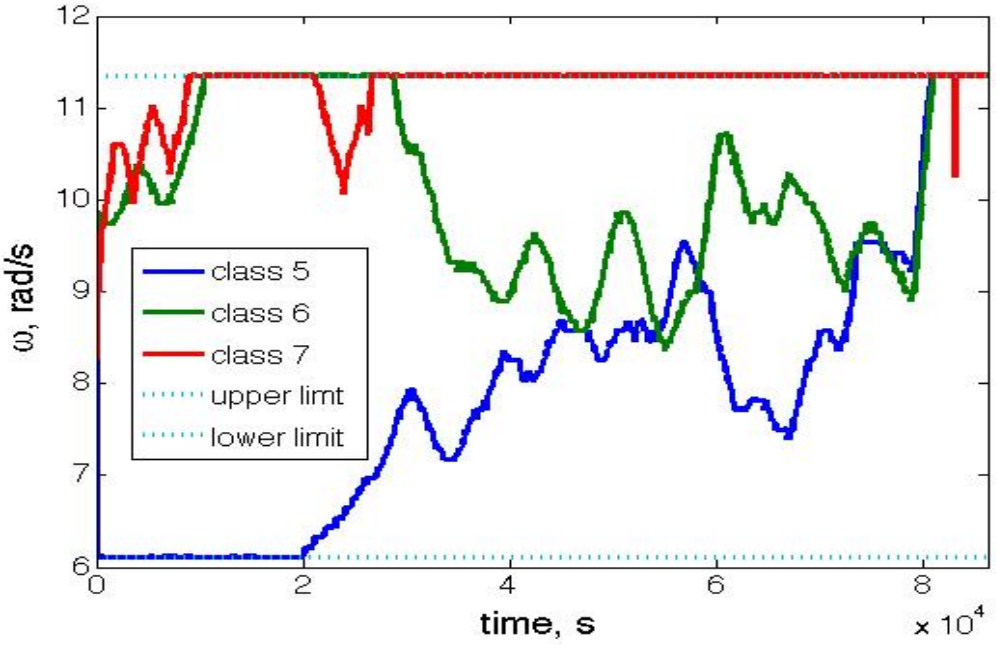


Figure 8: Plot of rotor angular velocity vs. time using the second version of the feedback control method.

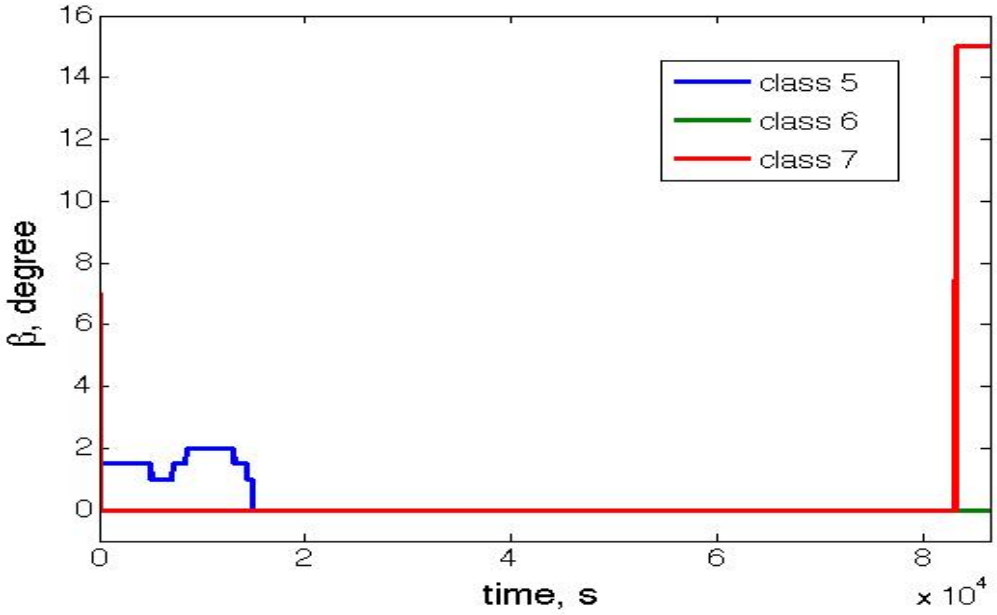


Figure 9: Plot of rotor pitch angle vs. time using the second version of the feedback control method.

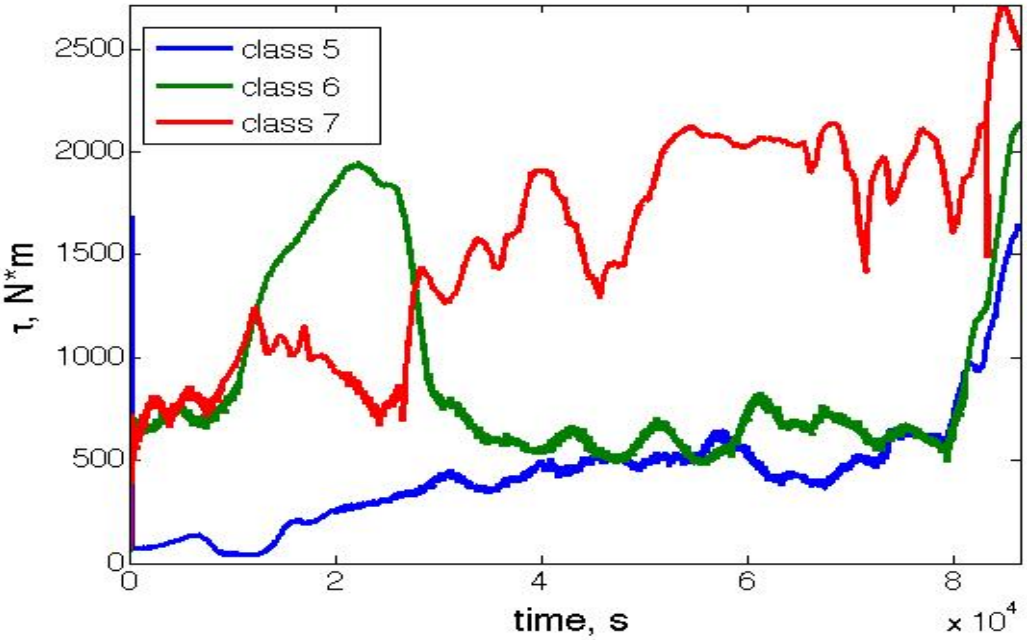


Figure 10: Plot of generator input torque vs. time using the second version of the feedback control method.

## COMPARISON OF SIMULATION RESULTS

The feedback control method is mainly used for 'Region 2' control for modern wind turbine systems, which has a relative low wind speed input; so the only comparison of the $C_p$ curves generated using these two modified feedback control methods will be made with the class 5 wind speed input.

For the first modified feedback control method, there is a region in which the power coefficient $C_p$ has very low values before the global maximum value is reached. When the global maximum can be reached, there is not big difference for the $C_p$ curves generated using these two methods. The $C_p$ curves when the global maximum can't be reached are compared in Figure 11.

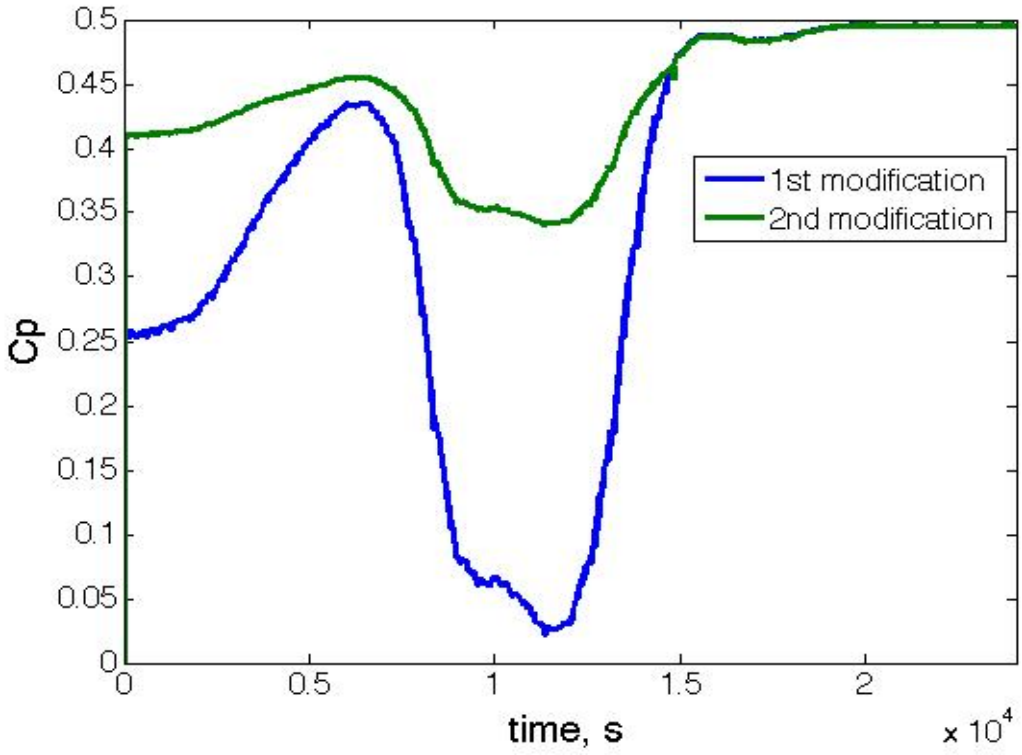


Figure 11: Comparison of the power coefficient curves using different versions of the modified feedback control methods.

From Figure 11, it is possible to see that before the global maximum value of $C_p$ can be reached, the performance of the second version of the modified feedback control method is much better than the first version. Even though the modified feedback control algorithm could harvest much more wind energy than the traditional feedback control algorithm does, it is unclear how close it is to the maximum energy capture. Optimization control strategies should be implemented to demonstrate the potential for wind energy harvesting.

# Chapter 5: *Direct shooting method*

Direct shooting method is a kind of numerical optimal control method [17-22], which finds the optimal solution to a given problem. There are also other numerical methods for optimal control, like the collocation method and the multiple-shooting method. Among them, the direct shooting method is the most commonly used one.

## PROBLEM FORMULATION

A general optimal control problem has the following form:

$$\min \ J = \phi(t_f, x_f) \tag{18}$$

$J$ is the performance index we want to minimize, subjected to the differential constraints:

$$\dot{x} = f(t, x, u) \tag{19}$$

and the following initial and final conditions and constraints:

$$t_0 = 0 \tag{20}$$

$$x_0 = x_{0_s} \tag{21}$$

$$\psi(t_f, x_f) = 0 \tag{22}$$

$$\theta(t_f, x_f) \leq 0 \tag{23}$$

$x_{0_s}$ stands for the initial value of x, which is specified. The control and state inequality constraints must also be satisfied:

$$C(t, x, u) \leq 0 \tag{24}$$

$$S(t, x, u) \leq 0 \tag{25}$$

**SUBOPTIMAL CONTROL PROBLEM**

To use numerical methods to solve an optimal control problem, it is necessary to convert a general optimal control problem of the form through Equations (18) to (25) into a parameter optimization problem. Conversion of optimal control problems into parameter optimization problems [18] is accomplished by replacing the control and state histories by control and state parameters and forming the histories by interpolation. Then a nonlinear programming algorithm like SQP method can be used to solve the parameter optimization problem.

First, the final time must be normalized as shown in Equation (26):

$$\tau = \frac{t}{t_f} \tag{26}$$

thus, when $t = 0,\ \tau = 0$; when $t = t_f,\ \tau = 1$.

The general form of an optimal control problem shown in Equations (12) to (19) can be written in a parameter optimization form:

$$\min\ J = \phi(t_f, x_f) \tag{27}$$

From Equations (19) and (26), the differential constraints become:

$$\frac{dx}{d\tau} = t_f \cdot f(t_f, \tau, x(\tau), u(\tau)) = g(\tau, x, u, t_f) \tag{28}$$

The prescribed initial conditions become:

$$\tau_0 = 0 \tag{29}$$

$$x_0 = x_{0_s} \tag{30}$$

and the final conditions and constraints become:

$$\tau_f = 1 \tag{31}$$

$$\psi(t_f, x_f) = 0 \tag{32}$$

$$\theta(t_f, x_f) \leq 0 \tag{33}$$

**PARAMETERIZE THE CONTROLS**

Figure 12 and 13 show how the controls are parameterized at nodes. In Figure 12, the final time is normalized using 5 nodes. Between nodes, the controls can be represented by various splines. For the simplest case, a linear interpolation is used, which can guarantee that the control constraints are satisfied. In Figure 13, a linear interpolation of the control over $\tau_k$ and $\tau_{k+1}$ has the form shown in Equation (34):

$$u = u_k + \frac{u_{k+1} - u_k}{\tau_{k+1} - \tau_k}(\tau - \tau_k) \tag{34}$$

If the controls at 2 nodes satisfy the control constraints, a linear interpolation of them will also satisfy the control constraints.

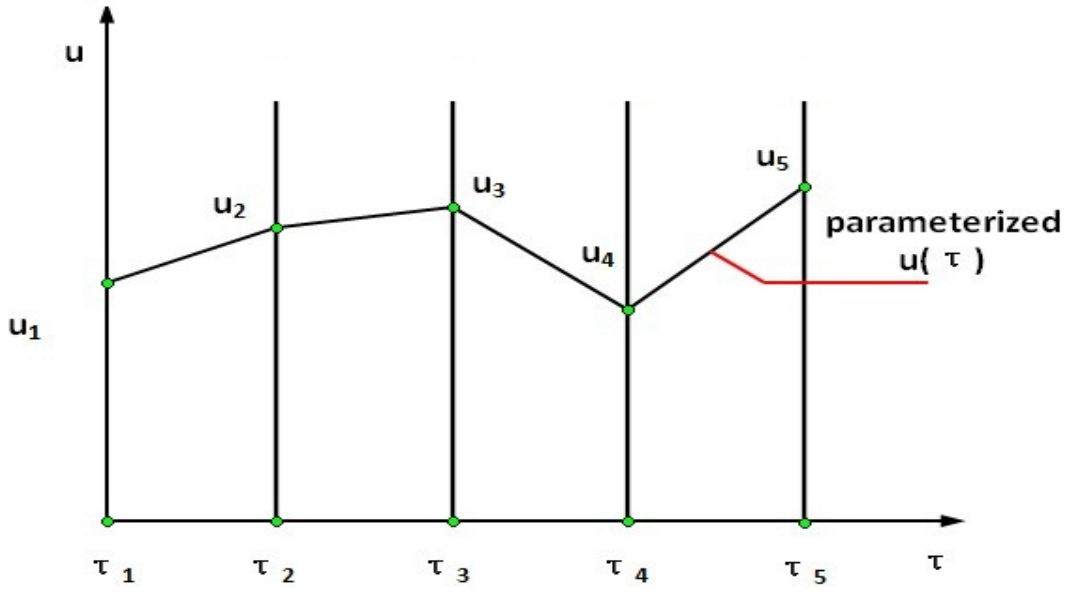


Figure 12: Parameterized control at nodes

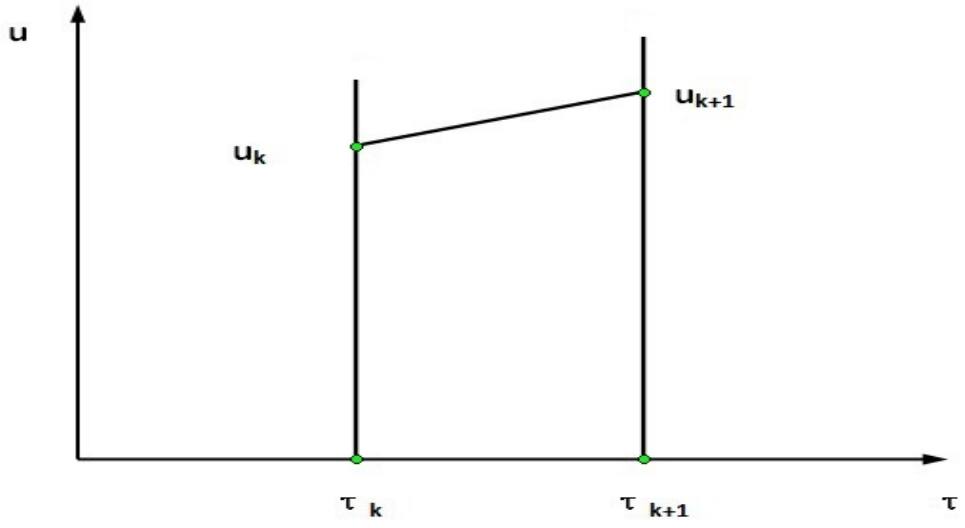


Figure 13: Linear interpolation of control between nodes

**ALGORITHM**

For a general optimal control problem with undetermined final time, the following steps are required to find the solution:

1. Guess values for $t_f$ and optimal control profiles at nodes: $u_1$, $u_2$ through $u_N$.

2. Integrate the differential equations which describes the system dynamics,

$$\frac{dx}{d\tau} = g(\tau, x, u_1, u_2, ..., u_N, t_f)$$

from $\tau_0$=0, $x_0$=$x_{0_s}$ to $\tau_f$=1 using a numerical integrator to obtain:

$$x_f = x_f(t_f, u_1, u_2, ..., u_N)$$

3. Performance index and constraints become:

$$J = \phi(x_f(t_f, u_1, u_2, ..., u_N), t_f) \coloneqq f(t_f, u_1, u_2, ..., u_N)$$
$$\psi(x_f(t_f, u_1, u_2, ..., u_N), t_f) = 0 \coloneqq c_i(t_f, u_1, u_2, ..., u_N) = 0,\ i = 1,2,...,m_e$$
$$\theta(x_f(t_f, u_1, u_2, ..., u_N), t_f) \le 0 \coloneqq c_i(t_f, u_1, u_2, ..., u_N) = 0,\ i = m_e + 1,...,m$$

where $m_e$ is the number of equality constraints, m is the total number of constraints.

Define parameter vector as:

$$X = [t_f, u_1, u_2, ..., u_N]^T$$

thus, the optimal control problem will become:

$$\min\ J = f(X)$$

subjected to:

$$c_i(X) = 0,\ i = 1,2,...m_e$$
$$c_i(X) \le 0,\ i = m_e + 1,...,m$$

This is a standard form of a nonlinear programming problem. As mentioned above, various nonlinear programming toolbox is suitable for solving this kind of problem.

**EXPLICIT RK INTEGRATOR**

A numerical integrator is needed to integrate the equations of motion. The most commonly used integrators are the series of Runge Kutta (RK) explicit integrators. Consider the system differential equations as:

$$\dot{x} = f(t, x, u)$$

Explicit means that all information necessary to compute *f* is known. Only fixed step integrators are considered.

The RK integrator has the following form:

$$\begin{aligned} x_{i+1} &= x_i + h\sum_{j=1}^{p} c_j f_j \\ f_1 &= f(t_i, x_i) \\ f_j &= f(t_i + h\alpha_j, x_i + h\sum_{\lambda=1}^{j-1} \beta_{j\lambda} f_\lambda), \quad j \ge 2 \end{aligned} \tag{35}$$

$p$ is the number of function evaluations to be used, $c$, $\alpha$ and $\beta$ are constants to be determined. To determine the values of the constants, $c$, $\alpha$ and $\beta$, we need to first specify $p$ and assume h is small, then expand the RK assumption in a Taylor-Series (TS) and compare the RK expansion with the exact TS expansion.

The exact TS expansion is given as follows:

$$x_{i+1} = x(t_i + h) = x(t_i) + \dot{x}(t_i)h + \frac{1}{2!}\ddot{x}(t_i)h^2 + \cdots \tag{36}$$

where,

$$\dot{x}(t_i) = f(t_i, x_i) \tag{37}$$

since,

$$\ddot{x} = f_t + f_x\dot{x} \tag{38}$$

we have:

$$\ddot{x}(t_i) = (f_t)_i + (f_x)_i(f)_i \tag{39}$$

For an nth order integrator, the RK TS matches the exact TS through terms of order $h^n$. Table 4 shows the $\alpha$ and $\beta$ values of the 4th order RK integrator.

| $\boldsymbol{\alpha_i}$ | $\boldsymbol{\beta_{ij}}$ |
|---|---|
| $\boldsymbol{\alpha_1} = 0$ | $\beta_{21} = \frac{1}{2}$ |
| $\boldsymbol{\alpha_2} = \frac{1}{2}$ | $\beta_{32} = \frac{1}{2}$ |
| $\boldsymbol{\alpha_3} = \frac{1}{2}$ | $\beta_{43} = 1$ |
| $\boldsymbol{\alpha_4} = 1$ | $\beta_{ij} = 0$ otherwise |

Table 4: $\alpha$ and $\beta$ values of the 4th order RK integrator

## NUMERICAL SIMULATION

Groups of simulations are performed to see if the optimal control algorithm works well on a modern wind turbine system. As mentioned above, a simple assumption is made that the wind speed remains constant every 1 minute. Thus, the final time of all the simulations is chosen to be 60 seconds. 7 nodes are used within the interval and the numerical integration method is chosen as the 4th order explicit RK integrator. The control and state constraints are already defined in Table 1. As discussed in Chapter 3, maximize wind energy capture is the same as maximize the power coefficient, $C_p$. Thus, we will define the performance index of this optimal control problem as Equation (40):

$$\max \quad J = \int_{t_0}^{t_f} C_p(\lambda(t), \beta(t))\, dt \tag{40}$$

subjected to the following initial and final conditions and constraints:

$$
\begin{aligned}
& t_0 = 0 \\
& t_f = 60 \\
& \omega_0 = \frac{1}{2}(\omega_{\max} + \omega_{\min}) \\
& \dot{\omega} = \frac{1}{J}(\frac{\pi}{8} D_r^2 \rho_{air} C_p \frac{V_w^3}{\omega} - \tau G_r) \\
& \omega_{rotor_{\min}} \le \omega_{rotor} \le \omega_{rotor_{\max}} \\
& \beta_{rotor_{\min}} \le \beta_{rotor} \le \beta_{rotor_{\max}} \\
& 0 < \tau_{generator} \le \tau_{\max}
\end{aligned}
\tag{41}
$$

the integration step of the 4th order RK integrator is chosen to be:

$$\Delta\tau = 1/60 \tag{42}$$

and there will be 10 integration steps within each interval. Then the general optimal control problem is converted to the form of a standard nonlinear programming problem and numerical methods are applied to find the solution.

**SIMULATION RESULTS**

Several groups of simulations are performed to evaluate the performance of the direct shooting method under different wind speed inputs. It is necessary to guess the optimal control profiles at nodes at the beginning of the simulation. Different initial guesses will lead to different solutions to the problem since the direct shooting method is a method to find the local minimum (or maximum) rather than the global minimum (or maximum). Seven nodes are used in the simulation and initial guesses of the rotor pitch angle, $\beta$ and the generator input torque, $\tau$ are vectors of length 7. In Figure 3, it is seen

that the power coefficient surface $C_p$ has many local minimums so a good initial guess of the controls is necessary for a satisfying solution.

One way to get a good initial guess is to refer to Figure 3. Every time wind speed changes; the range of $\lambda$ will also change. From Figure 3, we can roughly pick the $\beta$ value, which generates a local maximum value of $C_p$. The generator torque is roughly proportional to wind speed, so when wind speed grows bigger, a bigger initial guess of the generator torque is needed.

Figure 14 through 28 shows optimal trajectories under different wind speed profiles. For convenience, different wind speeds are randomly picked for the simulations. Each simulation lasts for 60 seconds during which the wind speed is assumed to be constant. The performance of the system is evaluated based on the $C_p$ curve generated.

The first group of simulations is performed under relative low wind speeds, which are 7, 10 and 12 *m/s*. When wind speed is relative small, according to Equation (10), the speed ratios $\lambda$ is relative large. According to Figure 3, when $\lambda$ falls into a proper range, the global maximum of $C_p$ is reachable; when $\lambda$ is too large or too small, the $C_p$ can only reach a local maximum.

Figure14 shows the plot of the power coefficient $C_p$ versus time for the first group of simulation. Figure 15 through 18 shows the corresponding plot of controls and states versus time. One can see that for all of these wind speed inputs, the pitch angle $\beta$ stays at 0° and high local maximums of $C_p$ are reached, which are almost 0.5. From

Figure 14, one can also see that the $C_p$ curve quickly reaches a local maximum value and then stays there. This is the kind of performance we expect to see.

Figure 16 shows the optimal generator input torque versus time. One can see that the generator input torque is roughly proportional to wind speed input. When wind speed increases, the optimal generator input torque also increases. The generator torque also reaches the steady state very quickly.

Figure 17 and 18 show the plot of the rotor angular velocity and the corresponding speed ratio versus time. It is seen that, the rotor speed is always in a proper range and never violate the constraint. Combining Figure 15, 18 and Figure 3, it's convenient to check if the optimal trajectory in Figure 14 is reasonable.

The second group of simulations is performed under medium wind speed inputs, which are 15, 18, 20 and 22 *m/s*. When wind speed is 15 *m/s*, $\lambda$ falls into an interval in which the local maximum value of $C_p$ is still close to 0.5. When wind speed increases from 18 to 22 *m/s*, the reachable local maximum of $C_p$ keeps decreasing.

For a wind speed input of 15, 18 and 20 *m/s*, the steady state value of $\beta$ is 0°, which means that all theses local maximums of $C_p$ lie on the curve with a zero degree of pitch angle in Figure 3. When wind speed is 22 *m/s*, which is large enough and makes $\lambda$ fall into the left part of the horizontal axis in Figure 3. This time, a different pitch angle will generate the local maximum of $C_p$.

Figure 21 shows the generator input torque for the second group of simulations. This time the generator input torque is not simply proportional to wind speed input. The input torque with a 20 *m/s* wind speed input is larger than that with a 22 *m/s* input.

The third group of simulations is performed under relative high wind speed inputs, which are 25, 28, and 30 *m/s*. According to Equation (10), the speed ratio, $\lambda$ will be small and fall into the left part of the horizontal axis in Figure 3. The corresponding global maximum value of $C_p$ is small. From Figure 24, it is seen that the $C_p$ values are very small under high wind speed inputs.

In Figure 25, pitch angles take large values, which correspond to the left portion of the local maximums in Figure 3. In Figure 26, it is seen that when wind speed input is really large, the generator input torque will also have large values.

After comparing all these groups of simulations, we can conclude that the direct shooting method performs well for the wind turbine operation. The optimal trajectory of $C_p$ will quickly reach a local maximum value and then stay there. The controls are states are in proper ranges and never violate the constraints.

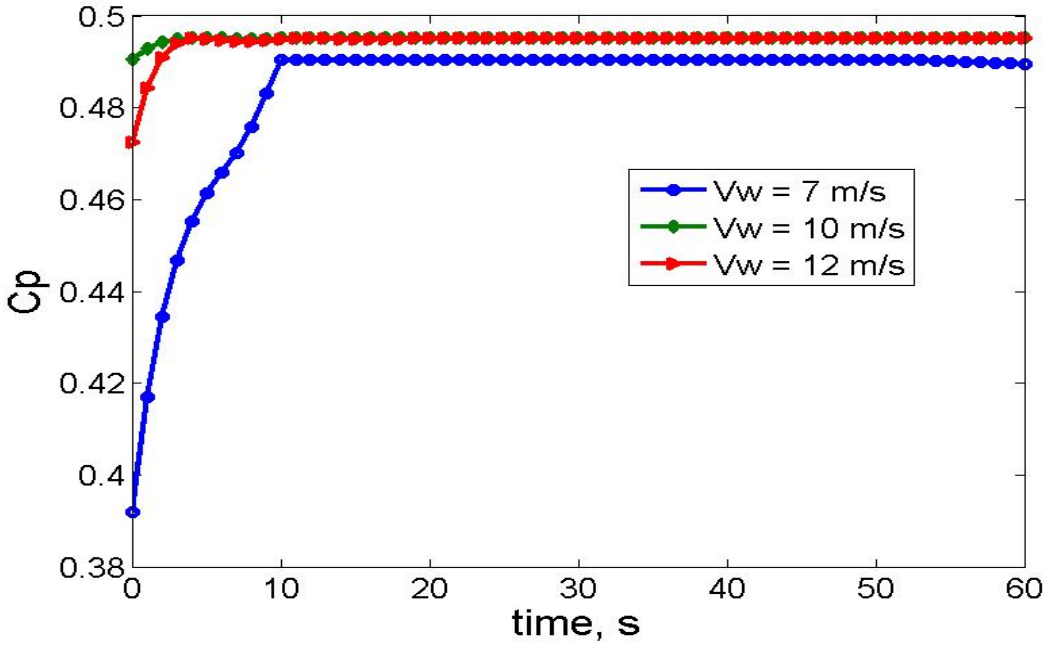


Figure 14: Plot of power coefficient vs. time using the direct shooting method with the first group of wind speed inputs.

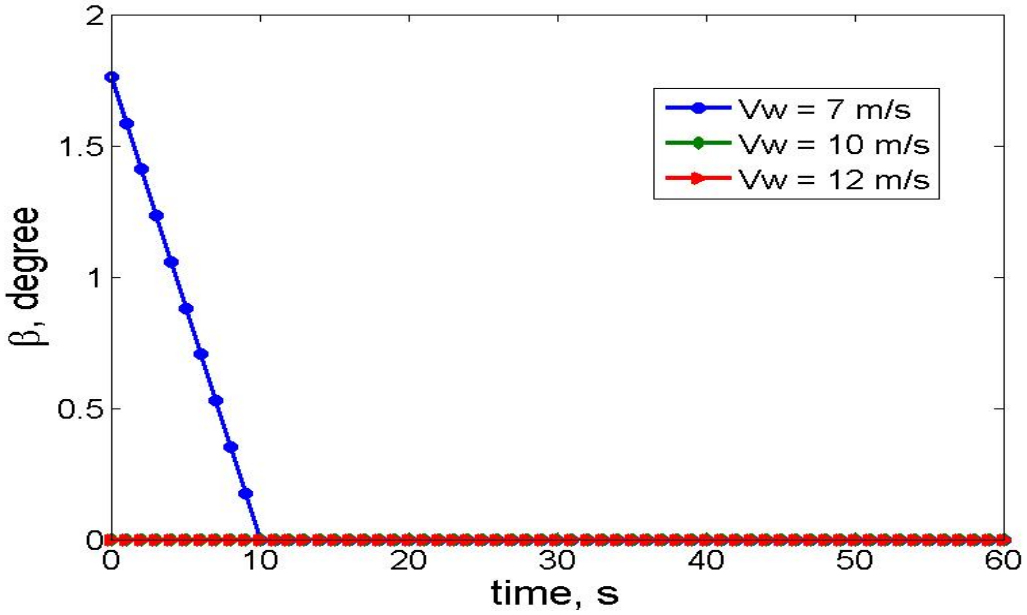


Figure 15: Plot of rotor pitch angle vs. time using the direct shooting method with the first group of wind speed inputs.

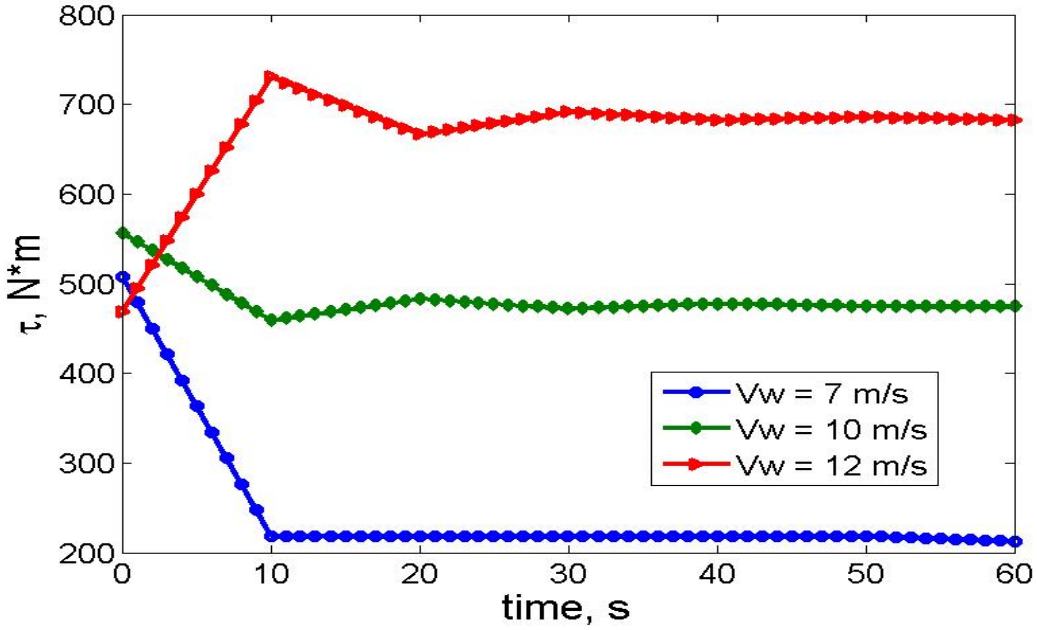


Figure 16: Plot of generator input torque vs. time using the direct shooting method with the first group of wind speed inputs.

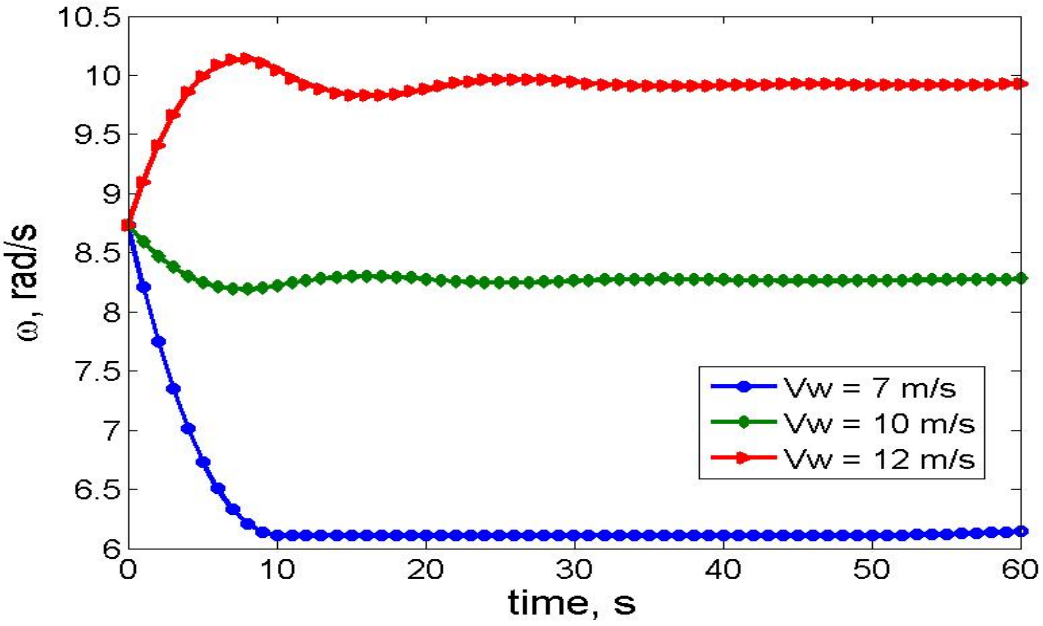


Figure 17: Plot of rotor angular velocity vs. time using the direct shooting method with the first group of wind speed inputs.

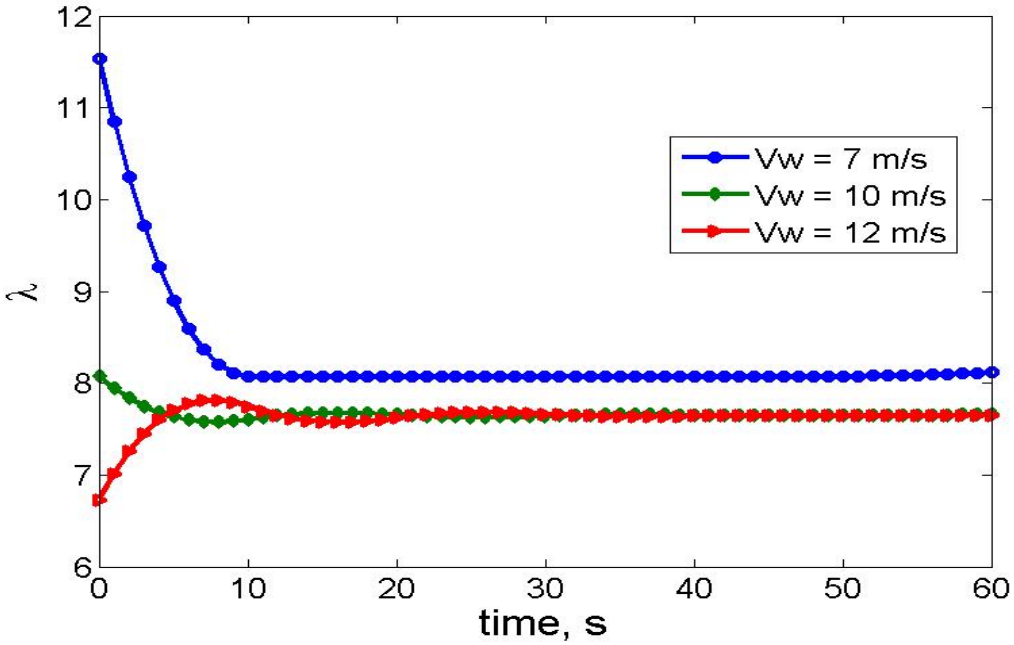


Figure 18: Plot of speed ratio vs. time using the direct shooting method with the first group of wind speed inputs.

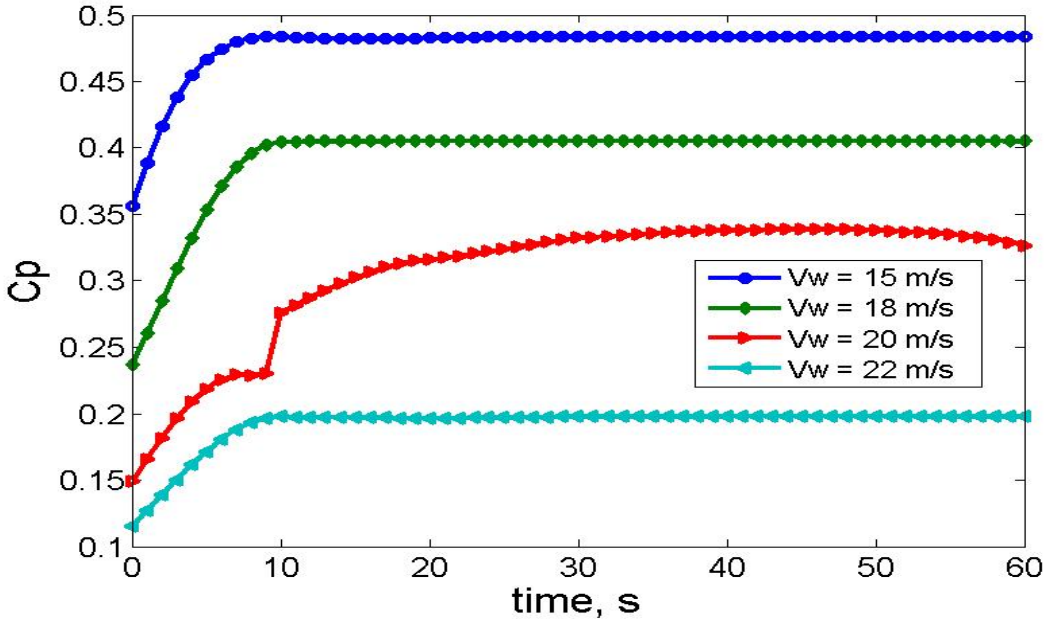


Figure 19: Plot of power coefficient vs. time using the direct shooting method with the second group of wind speed inputs.

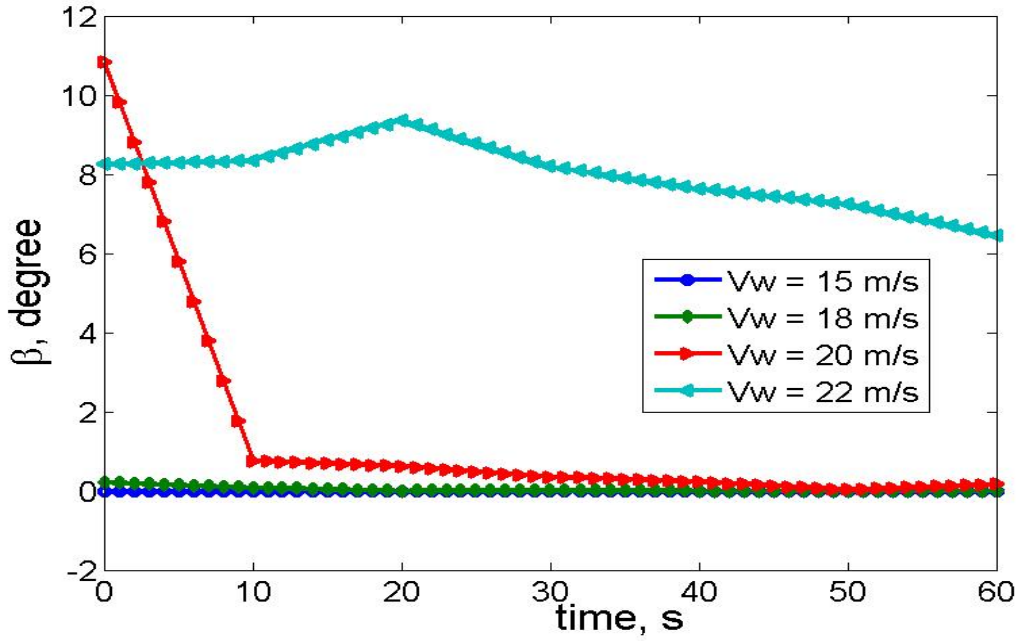


Figure 20: Plot of rotor pitch angle vs. time using the direct shooting method with the second group of wind speed inputs.

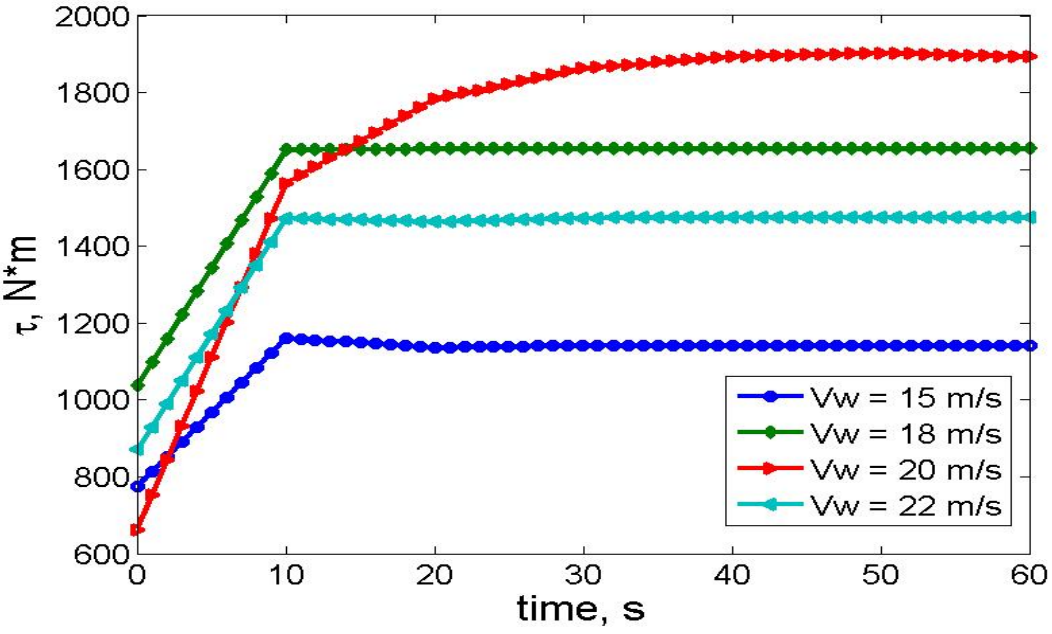


Figure 21: Plot of generator input torque vs. time using the direct shooting method with the second group of wind speed inputs.

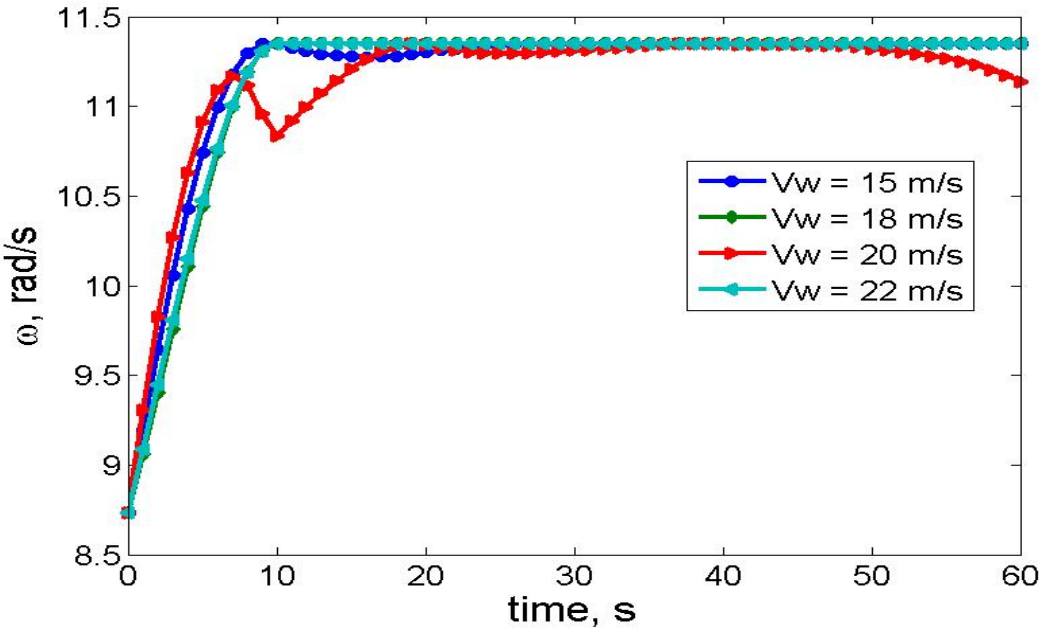


Figure 22: Plot of rotor angular velocity vs. time using the direct shooting method with the second group of wind speed inputs.

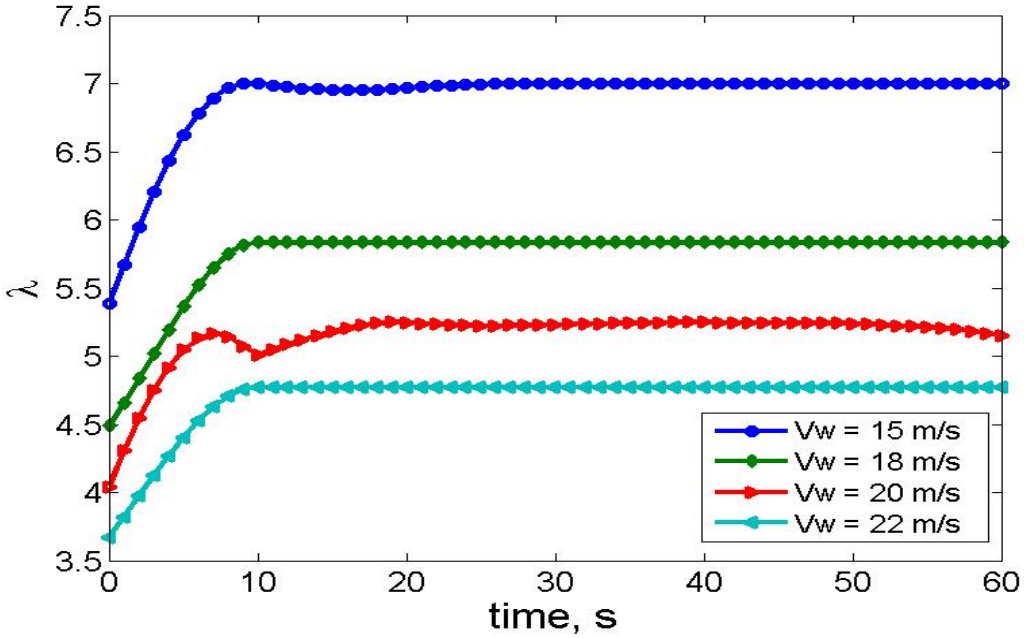


Figure 23: Plot of speed ratio vs. time using the direct shooting method with the second group of wind speed inputs.

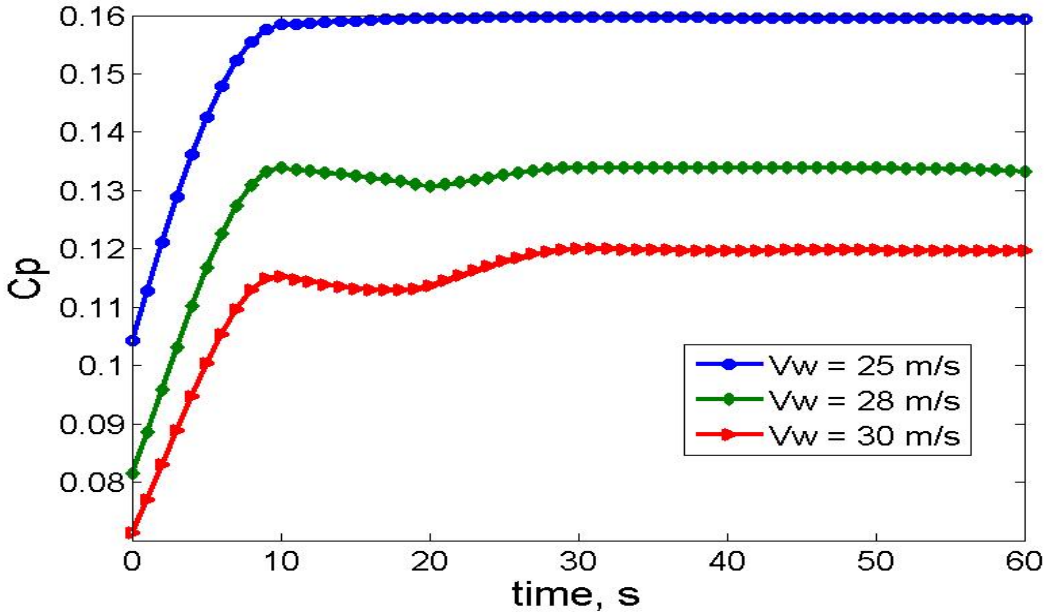


Figure 24: Plot of power coefficient vs. time using the direct shooting method with the third group of wind speed inputs.

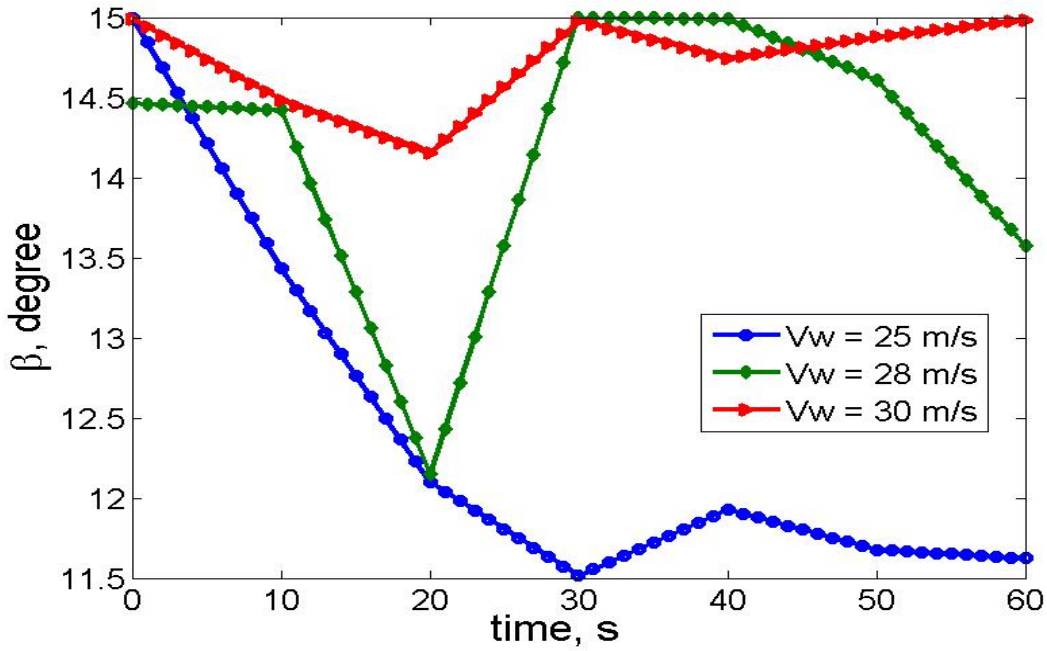


Figure 25: Plot of rotor pitch angle vs. time using the direct shooting method with the third group of wind speed inputs.

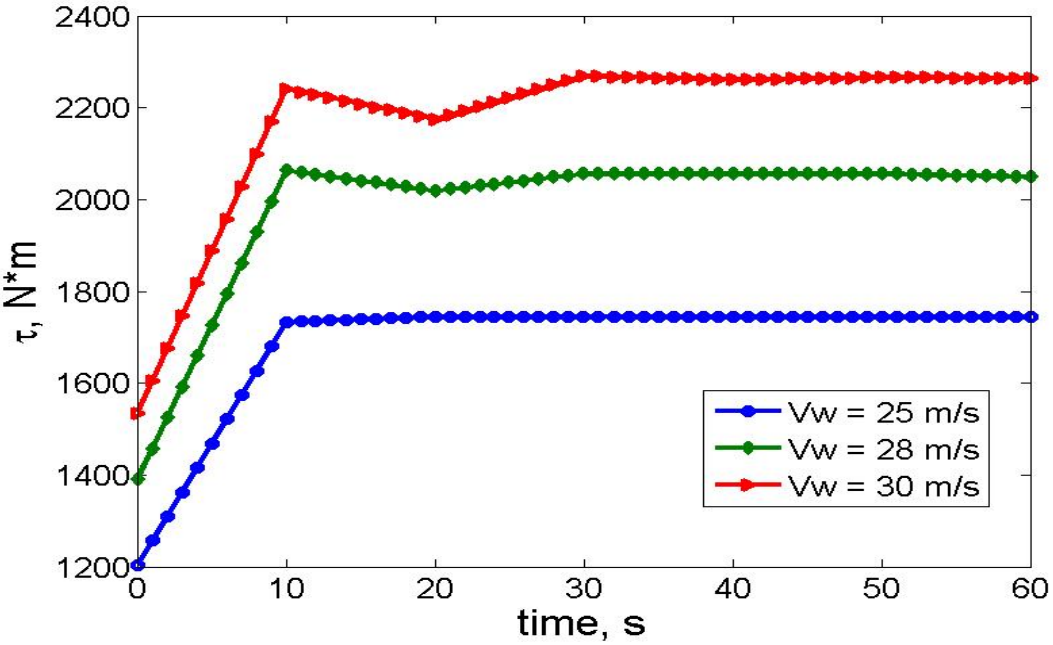


Figure 26: Plot of generator input torque vs. time using the direct shooting method with the third group of wind speed inputs.

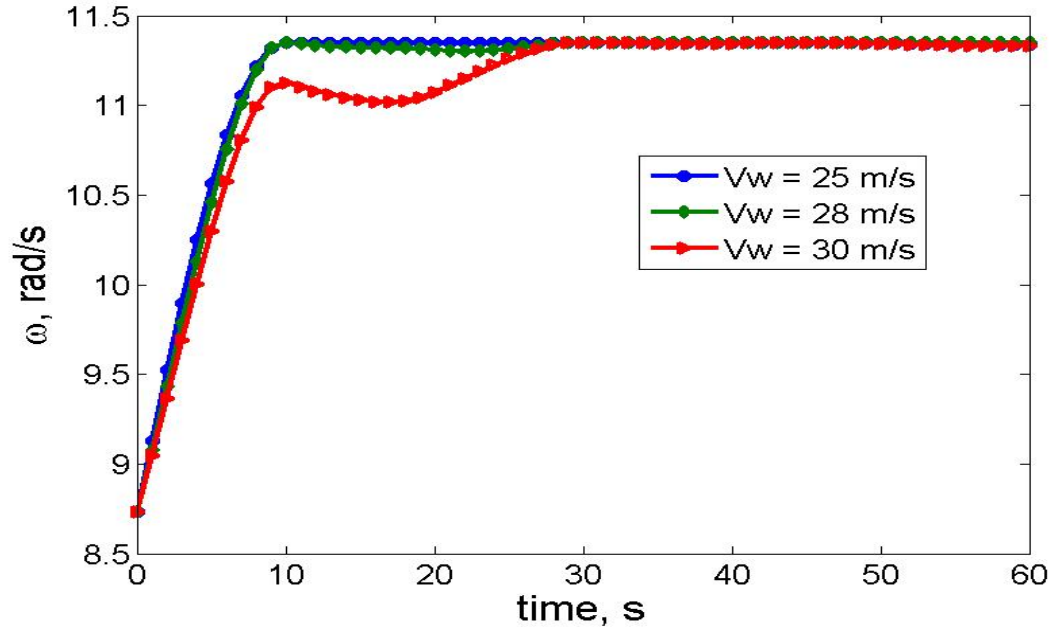


Figure 27: Plot of rotor angular velocity vs. time using the direct shooting method with the third group of wind speed inputs.

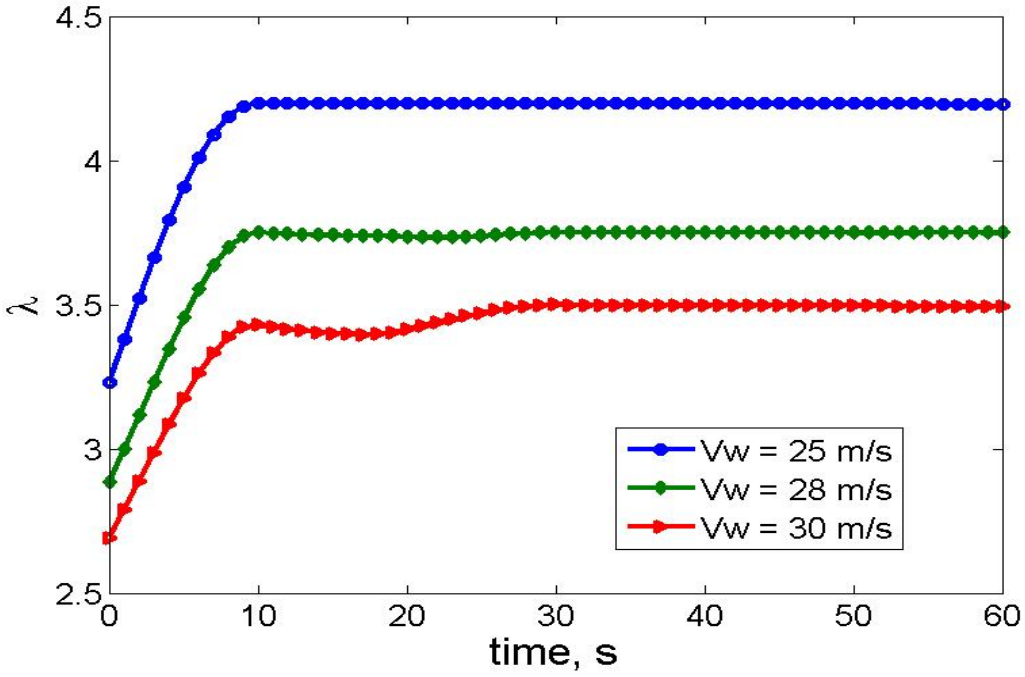


Figure28: Plot of speed ratio vs. time using the direct shooting method with the third group of wind speed inputs.

# Chapter 6: *Dynamic programming method*

Unlike the direct shooting method, the dynamic programming (DP) approach is another kind of numerical method, which finds the global optimal solution over a time horizon. For a given wind speed profile, the DP algorithm will help us to find the optimal trajectories of the input torque command and the rotor pitch angle which leads to the maximum wind energy capture.

## INTRODUCTION TO DYNAMIC PROGRAMMING

Dynamic programming is a method for solving complex problems by breaking them down into simpler subproblems [22]. The key idea behind dynamic programming is quite simple. In general, to solve a given problem, one needs to solve different parts of the problem (subproblems), then combine the solutions of the subproblems to reach an overall solution. Often, many of these subproblems are really the same. The dynamic programming approach seeks to solve each subproblem only once, thus reducing the number of computations: once the solution to a given subproblem has been computed, it is stored or 'memorized': the next time the same solution is needed, it is simply looked up. This approach is especially useful when the number of repeating subproblems grows exponentially as a function of the size of the input.

The formula of dynamic programming will differ for different problems, but the structure for the algorithm still remains the same. The following sections give a brief introduction to how to apply the DP algorithm to a modern wind turbine system. The main advantage of the DP algorithm over other numerical method is that a global optimal

solution can be found while using DP. Other numerical methods usually find the local optimal solutions.

**MODEL DISCRETIZAITON**

Since the DP approach is a numerical method, which involves the discretization of time and states, the performance index should also be written into a discretized form. We choose a discretized time step to be one second within every minute. The states are also discretized. In traditional DP approach, control inputs are discretized, which are the generator input torque and the rotor pitch angle. However, compared to the generator torque, the rotor angular velocity, which is the control input, has a smaller range. Thus, discretize the rotor angular velocity and then back calculate the input torque command that leads to the desired angular velocity will reduce the iterations and make the DP algorithm more efficient.

The discretization should satisfy all of the control and state constraints. When the time and state variables are well discretized, the performance index for the DP algorithm can be written into a discretized form:

$$\max J = \sum_{k=1}^{k_{\max}-1} \int_{t_k}^{t_{k+1}} C_p(\lambda_{k,k+1}(t), \beta_{k,k+1}(t))dt \tag{43}$$

We use each discretized time step as a node at which the rotor angular speed and pitch angle are both discretized. $k$ is the index of each node. We want to use the DP algorithm to find the optimal combinations of $\omega$ and $\beta$ at each node, which generates the maximum $C_p$ value, which leads to the maximum wind energy capture.

Functions $\omega(t)$ and $\beta(t)$ between nodes could be in a variety of forms. To make it simple, a linear interpolation is used. Combining the values of $\omega(t)$ and $\beta(t)$ at nodes, we have:

$$\begin{aligned}\omega(t) &= \omega_k + \frac{\omega_k - \omega_{k-1}}{t_k - t_{k-1}}(t - t_{k-1}) \\ \beta(t) &= \beta_k + \frac{\beta_k - \beta_{k-1}}{t_k - t_{k-1}}(t - t_{k-1})\end{aligned} \tag{44}$$

while $\omega(t)$ is known, $\lambda(t)$ can be derived from Equation (10). With $\lambda(t)$ and $\beta(t)$ known, Equation (43) can be integrated numerically. The linearly variation of the pitch angle in the form of Equation (44) can be directly controlled. Combining Equation (44) and Equation (8), the generator torque that must be applied to generate a linearly changing rotor angular velocity has the form of Equation (45):

$$\tau_{k,k+1}(t) = \frac{1}{G_r}\left(\frac{\pi}{8} D_r^2 \rho_{air} C_p\left(\frac{(\omega_k + \frac{\omega_k - \omega_{k-1}}{t_k - t_{k-1}}(t - t_{k-1}))D_r}{2V_w}, (\beta_k + \frac{\beta_k - \beta_{k-1}}{t_k - t_{k-1}}(t - t_{k-1})\right)\right. \\ \left.\frac{V_w^3}{(\omega_{k+1} - \omega_k)t - \omega_k} - J(\omega_{k+1} - \omega_k)\right) \tag{45}$$

Figure 29 is an intuitional picture shows the states at nodes and the form of functions between nodes. Since linear interpolation is used for $\omega(t)$ and $\beta(t)$ between nodes, constraints are guaranteed to be satisfied for values between nodes. However, the generator input torque between nodes, which has the form of Equation (45), may not satisfy the constraint. The solution to this problem is to eliminate the torque profiles

between nodes whose maximum value is greater than the upper limit or whose minimum value is smaller than the lower limit of the generator input torque.

The continuity of the functions are guaranteed by using the final conditions of the last interval as the initial conditions of the next interval, which can be expressed as:

$$\begin{aligned} \omega_{k-1,k}(t_k) &= \omega_{k,k+1}(t_k) \\ \beta_{k-1,k}(t_k) &= \beta_{k,k+1}(t_k) \\ \tau_{k-1,k}(t_k) &= \tau_{k,k+1}(t_k) \end{aligned} \tag{46}$$

thus, the DP algorithm can be well applied. As mentioned above, we will run the DP algorithm every 1-minute during which interval the wind speed input is assumed to be constant.

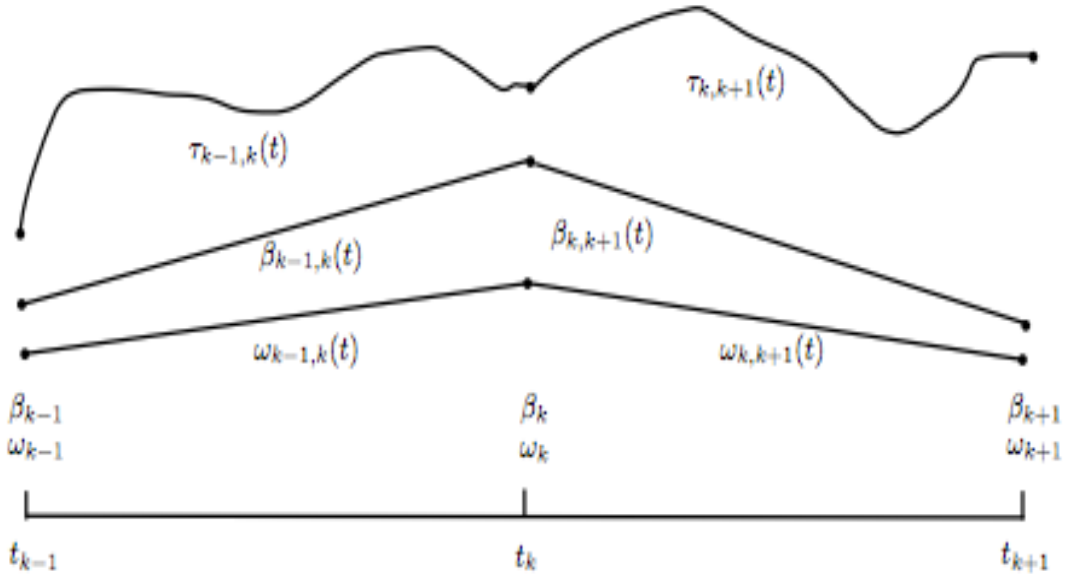


Figure 29. States discretization.

**SIMULATION RESULTS**

The DP analyzed the performance of various wind speed inputs and obtained a customized, optimal, solution for each case. For the reason of comparison, the same group of wind speed inputs for simulations of the direct shooting method is used. Figure 30 through 44 show all of the simulation results.

Figure 30 through 34 show the simulation results of the first group, whose wind speed inputs are relative low. According to Figure 30, it is seen that the $C_p$ curve always quickly reaches an optimal value and then stays there. Due to the character of the DP algorithm, one should expect that this optimal value is the best among all of the local optimums. When wind speed changes, the best local optimal value the system can reach differs. It is seen that when wind speed is 5 *m/s*, which is very low, the optimal $C_p$ value

the system can reach is about 0.4. When wind speed is 7, 10 and 12 *m/s*, the optimal $C_p$ value is very high, which is almost 0.5.

Figure 32 and 34 show the rotor pitch angle and the speed ratio corresponding to the optimal power coefficient trajectories. It is seen that when wind speed input is 7, 10 and 12 *m/s*, the rotor pitch angle, $\beta$ stays at 0° and the speed ratio $\lambda$ stays at about 8. In Figure 3, it is seen that a combination of the above $\beta$ and $\lambda$ values will generate a high $C_p$ value, which is almost 0.5. When wind speed is too small, like 5 *m/s*, $\lambda$ will fall into the right part of the horizontal axis in Figure 3. At this time, a 0° of pitch angle won't generate the best local optimal $C_p$ so $\beta$ becomes about 1.5° in Figure 32. Combining Figures 30, 32, 34 and Figure 3, one can see that the optimal trajectories generated by the DP algorithm are reasonable. Figure 31 show the plot of the generator input torque versus time. It is seen that as wind speed increases, the generator torque will also increase.

Figure 35 through 39 show the simulation results of the second group, whose wind speed inputs are medium. From Figure 35, it is seen that as wind speed increase, the optimal $C_p$ value will decrease. In Figure 37, $\beta$ stays at 0° for all of the 4 wind speed inputs, which means all of the optimal $C_p$ values lie on the curve of $\beta = 0$ in Figure 3. Figure 36 shows the generator input torque corresponding to the optimal trajectories. It is also seen that the generator input torque increases as wind speed increases.

Figure 40 through 44 show the simulation results of the third group. In Figure 42, it is seen that when wind speed is large enough, for example, over 28 *m/s*, a 15° of the rotor pitch angle will generate the optimal $C_p$ value. In Figure 3, it is seen that when wind speed is large enough, $\lambda$ will fall into the very left part of the horizontal axis and a

25° of $\beta$ will generate a local optimum of $C_p$. Since the upper limit of $\beta$ is 15° in the simulation, 15° will be used instead of 25°. Figure 41 shows the plot of the generator input torque versus time corresponding to the third group of simulations. It is seen that the generator input torque with a 25 *m/s* wind speed input is greater than that with a 28 *m/s* wind speed input.

All of the conclusions drawn from the simulation results using the DP method converge with those drawn from the direct shooting method.

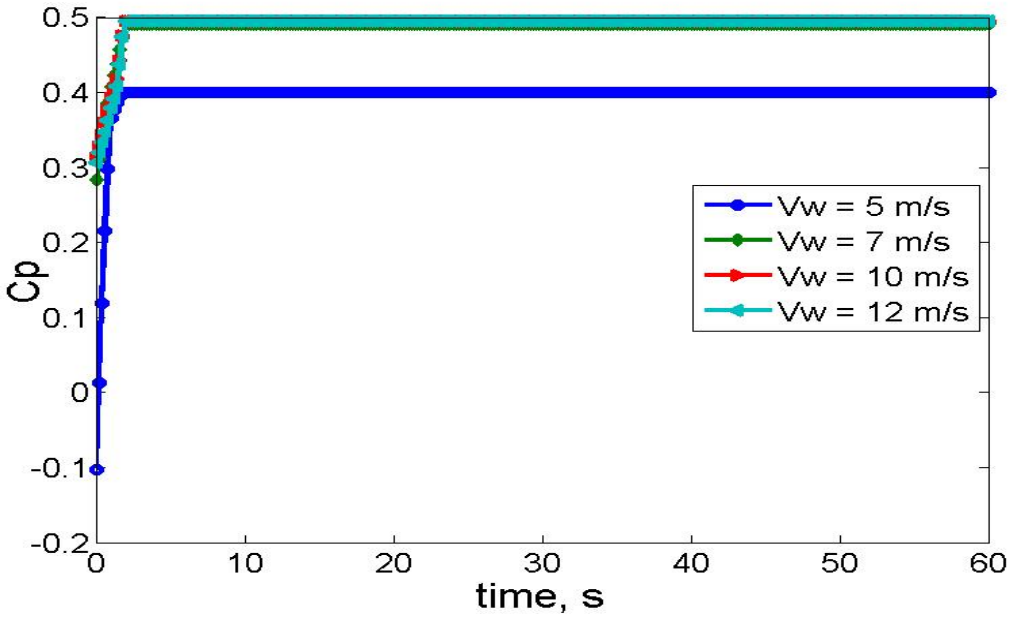


Figure 30: Plot of power coefficient vs. time using the DP method with the first group of wind speed inputs.

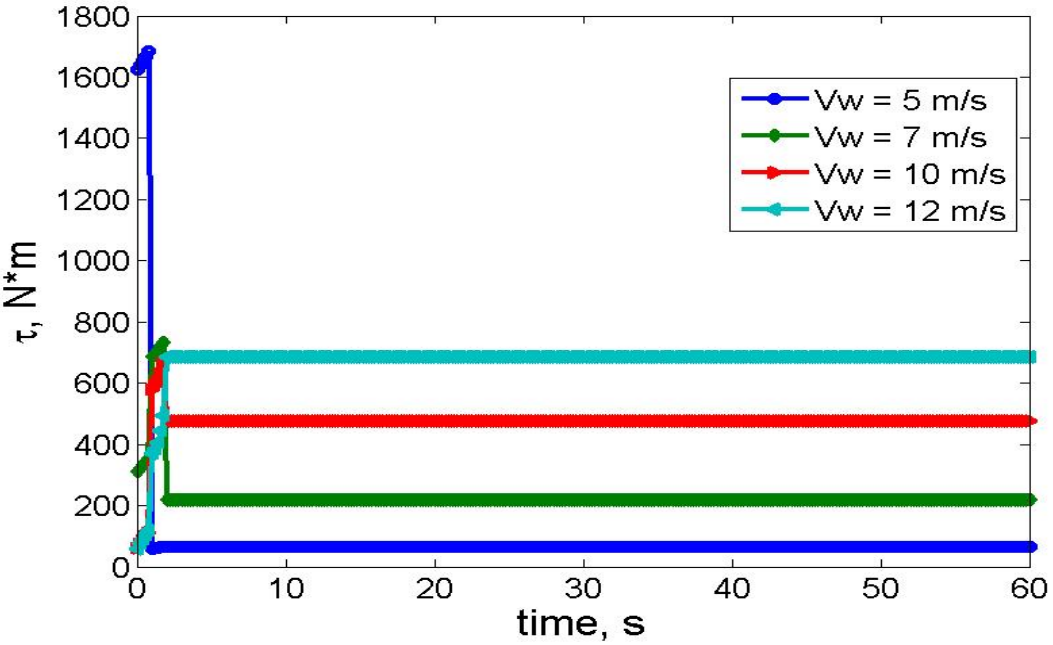


Figure 31: Plot of generator input torque vs. time using the DP method with the first group of wind speed inputs.

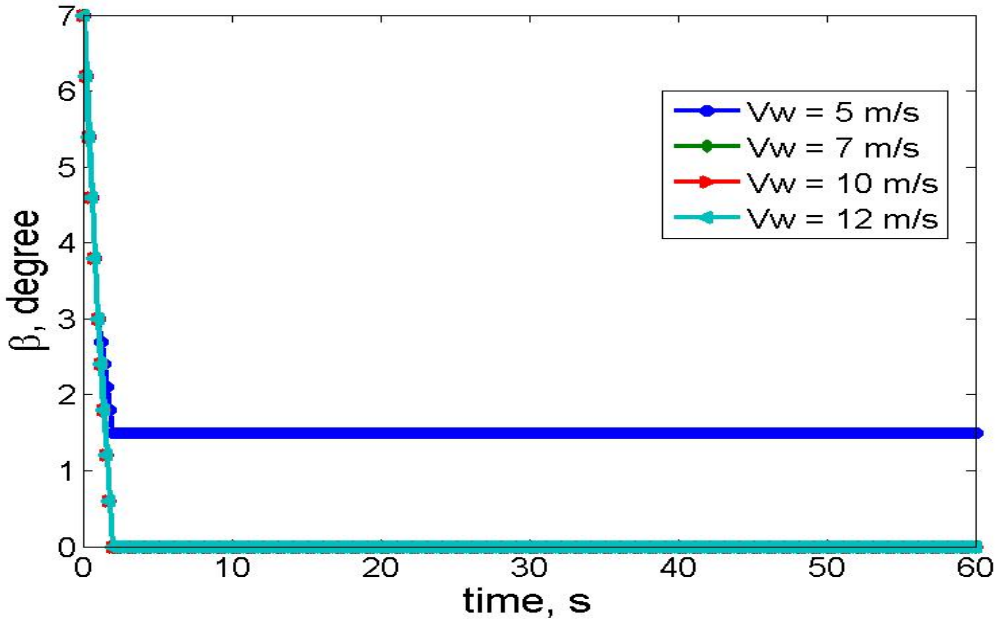


Figure 32: Plot of rotor pitch angle vs. time using the DP method with the first group of wind speed inputs.

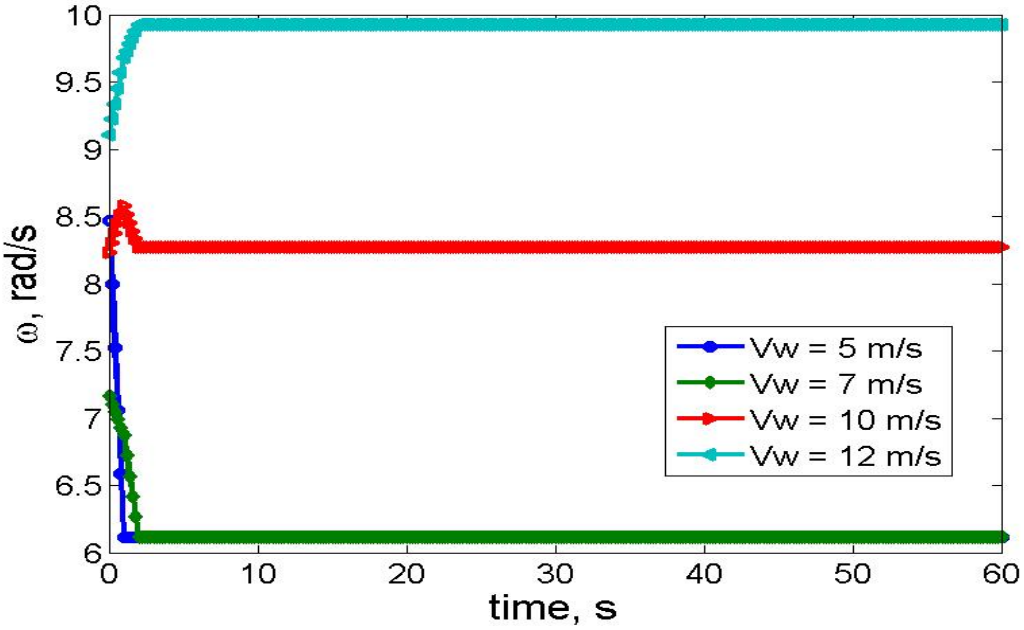


Figure 33: Plot of rotor angular velocity vs. time using the DP method with the first group of wind speed inputs.

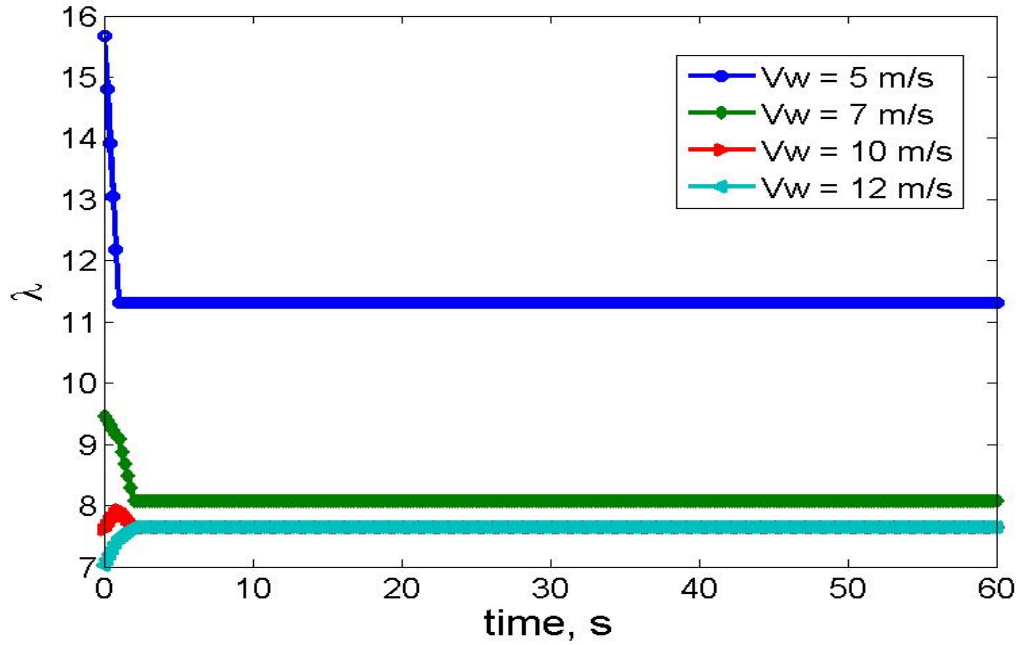


Figure 34: Plot of speed ratio vs. time using the DP method with the first group of wind speed inputs.

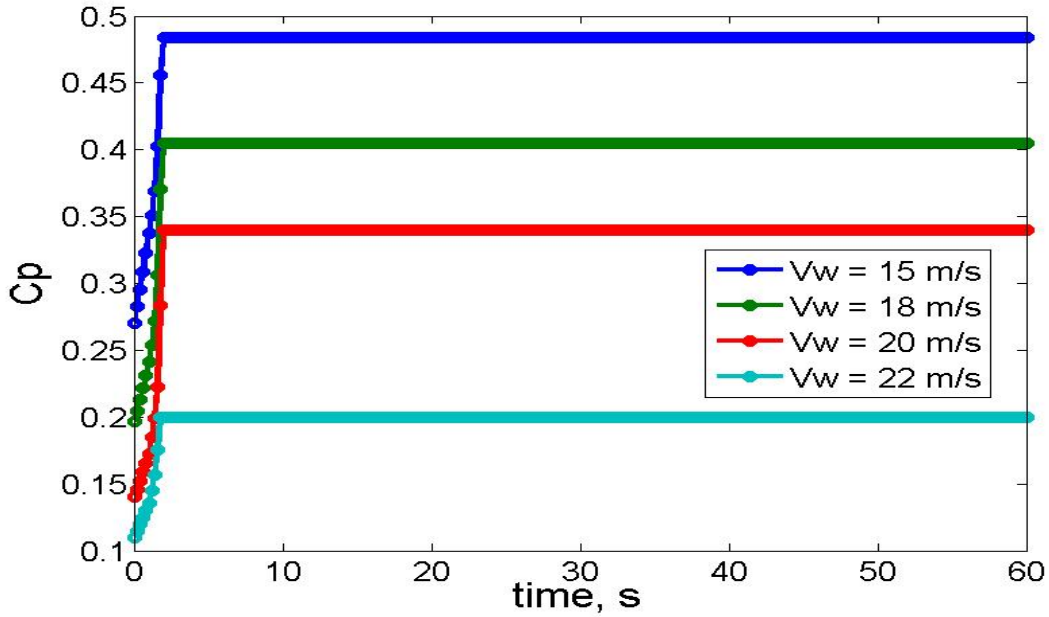


Figure 35: Plot of power coefficient vs. time using the DP method with the second group of wind speed inputs.

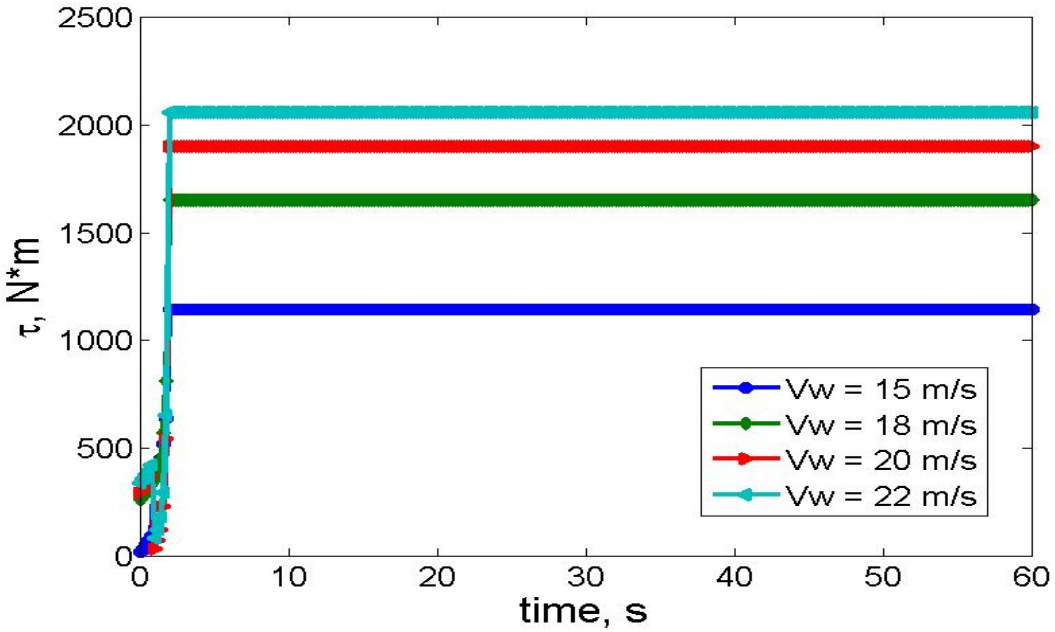


Figure 36: Plot of generator input torque vs. time using the DP method with the second group of wind speed inputs.

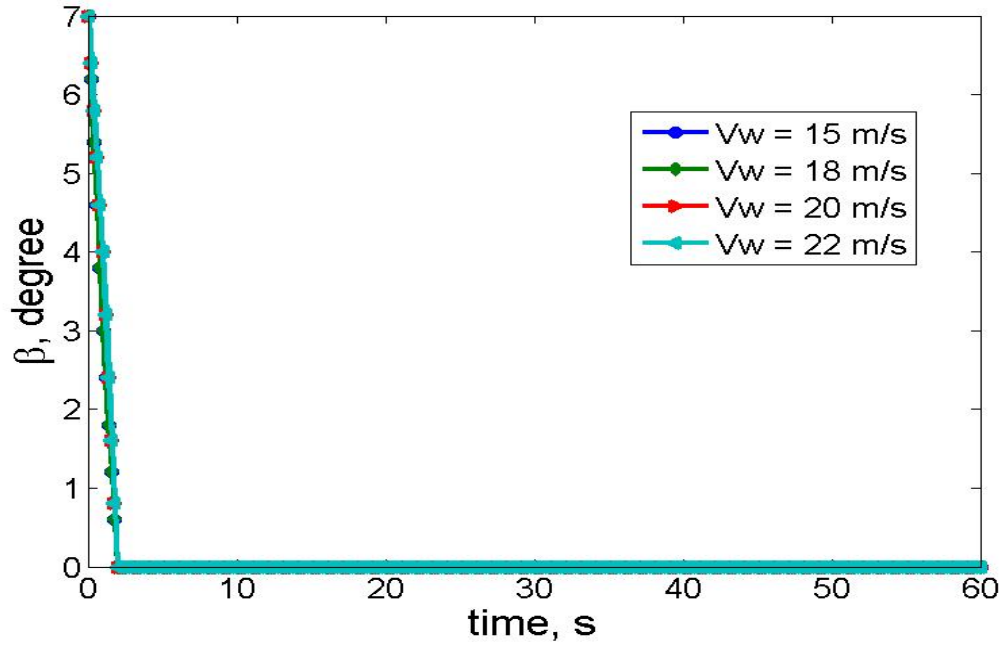


Figure 37: Plot of rotor pitch angle vs. time using the DP method with the second group of wind speed inputs.

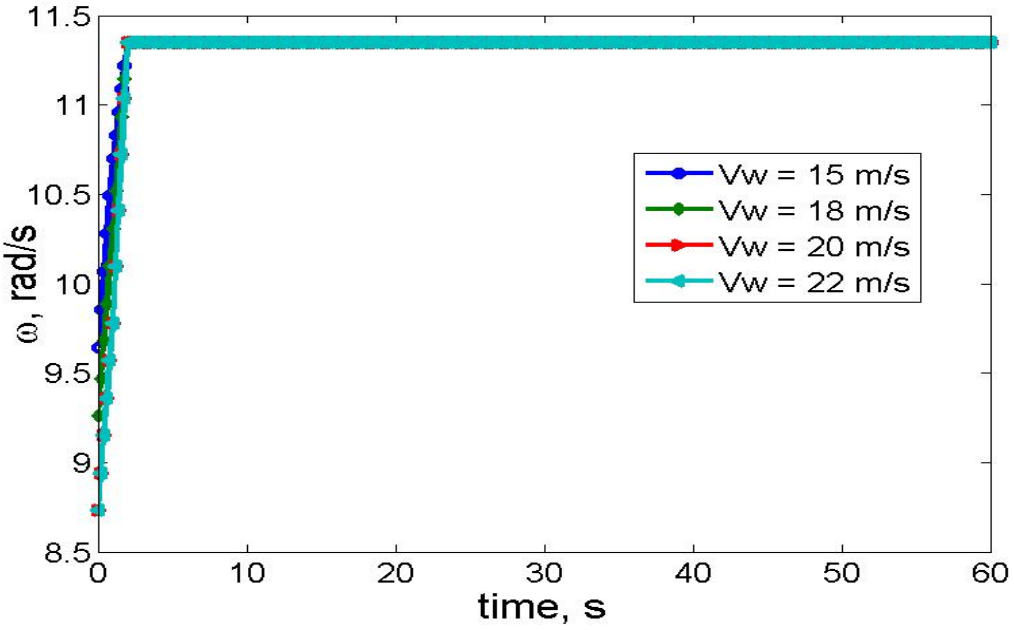


Figure 38: Plot of rotor angular velocity vs. time using the DP method with the second group of wind speed inputs.

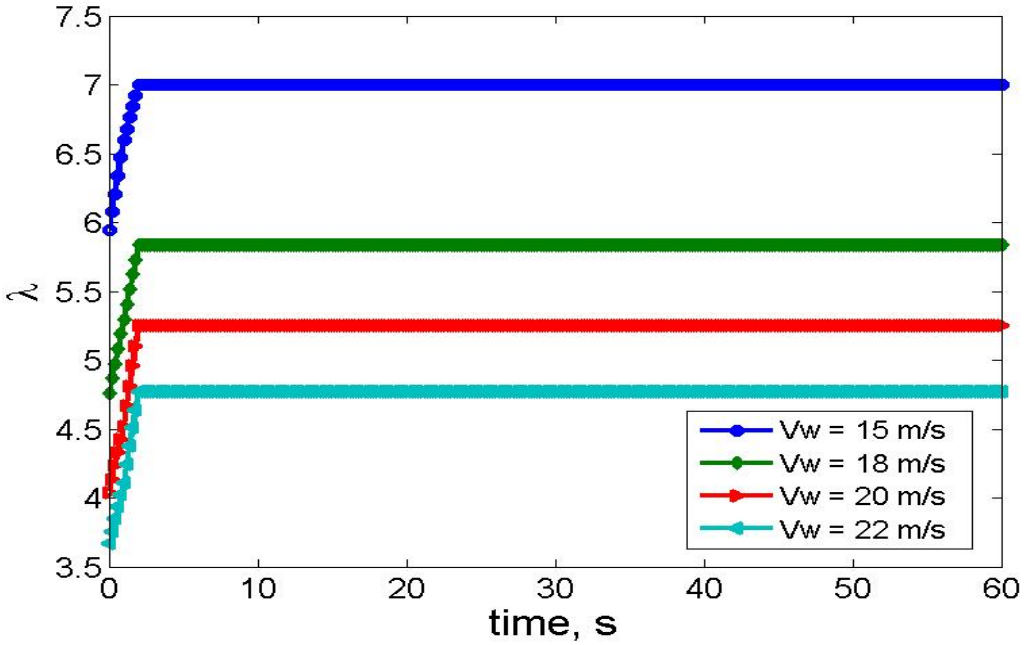


Figure 39: Plot of speed ratio vs. time using the DP method with the second group of wind speed inputs.

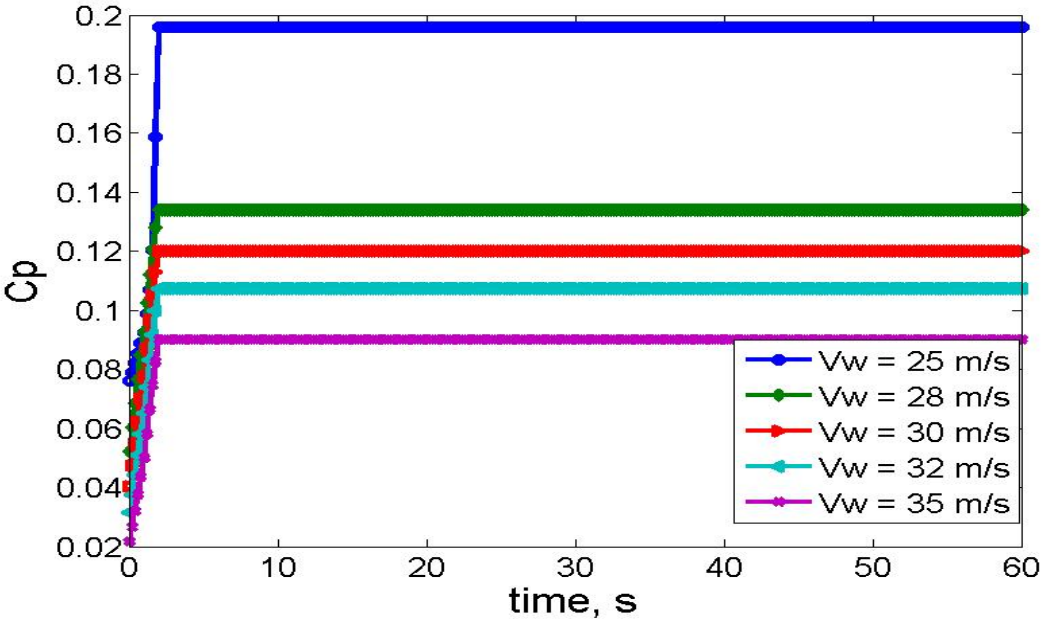


Figure 40: Plot of power coefficient vs. time using the DP method with the third group of wind speed inputs.

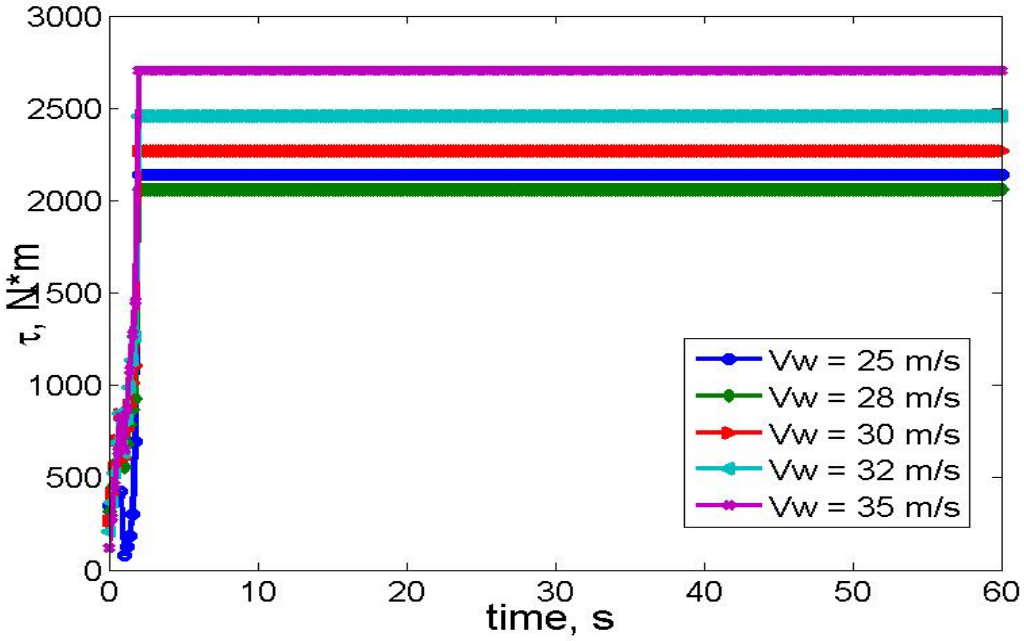


Figure 41: Plot of generator input torque vs. time using the DP method with the third group of wind speed inputs.

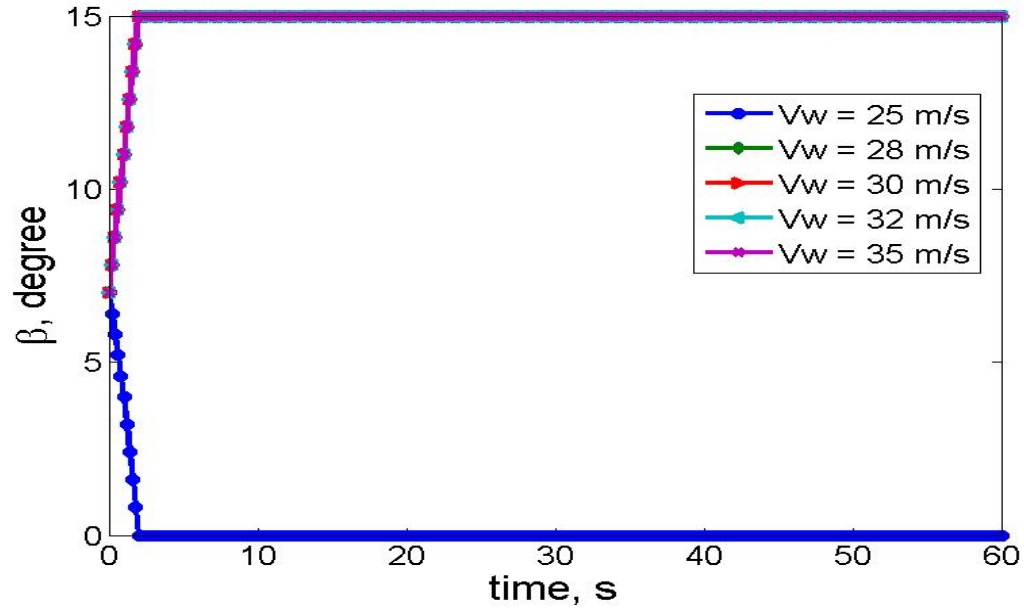


Figure 42: Plot of rotor pitch angle vs. time using the DP method with the third group of wind speed inputs.

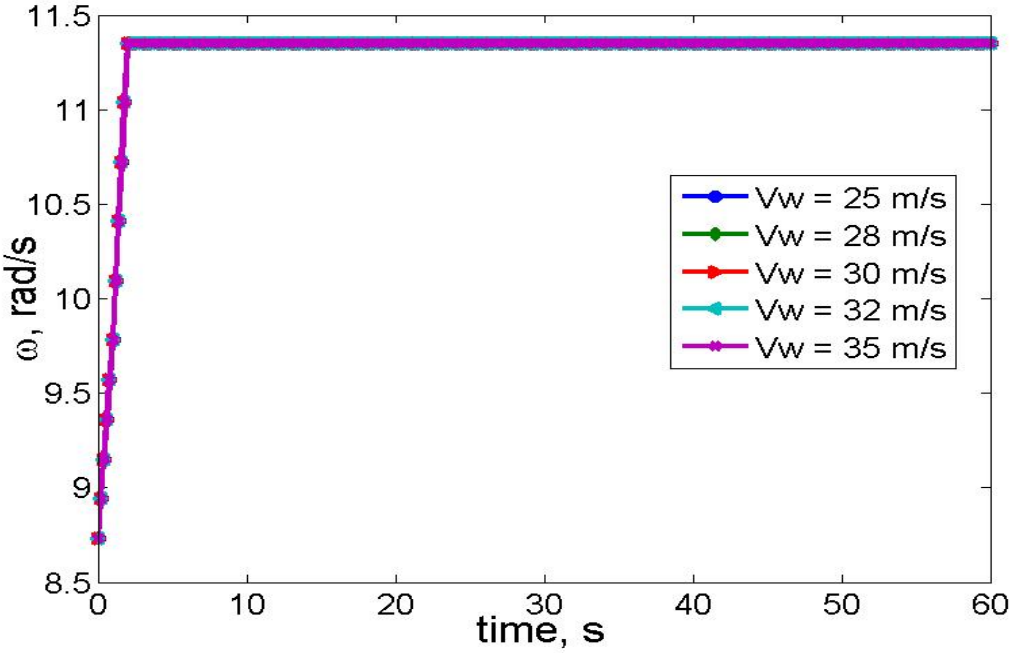


Figure 43: Plot of rotor angular velocity vs. time using the DP method with the third group of wind speed inputs.

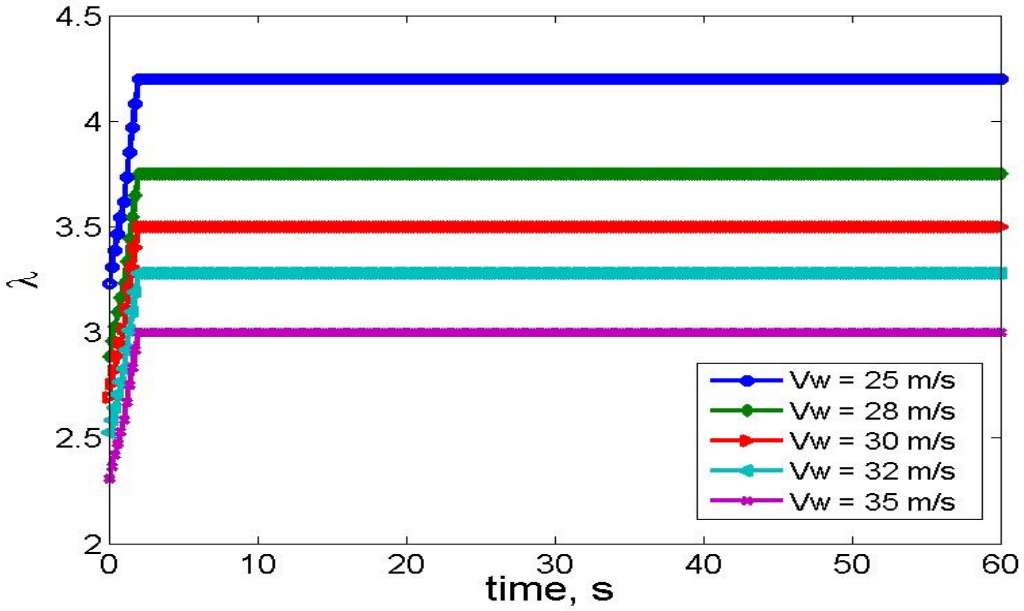


Figure 44: Plot of speed ration vs. time using the DP method with the third group of wind speed inputs

# Chapter 7: *Comparison of control methods*

## COMPARISON BETWEEN DIRECT SHOOTING AND DP

Frist of all, a comparison between the direct shooting method and the dynamic programming (DP) method is considered. As mentioned in Chapter 5, the optimal solution generated by the direct shooting method is greatly affected by the initial guesses of the control profiles. Back to all of the simulation results generated under different wind speed inputs in Chapter 5, the group of simulations with a 15 *m/s* wind speed input is relative satisfying and will be used to compare to the simulation result generated by the DP algorithm also with the same wind speed input.

Figure 45 through 49 show the comparison plots of the different control methods with the same wind speed of 15 m/s. Figure 45 shows the comparison plot of the power coefficient versus time. From the plot, it is seen that the $C_p$ curves generated by these two different methods reach the same steady state value. The only difference is that the $C_p$ curve generated by the DP method reaches the steady state value more quickly than the curve generated by the direct shooting method. This may be cause by that smaller integration steps are used in the DP method than the direct shooting method.

Figure 46 through 49 show the corresponding comparison plots of control and states versus time. Generally, all of the controls and states generated by theses two different methods reach the same steady state value and the DP method has a quicker response than the direct shooting method.

Figure 50 through 54 shows another group of comparison plot using a wind speed input of 25 $m/s$, which is relative high. This time, it is seen that the performance of the DP method is much better than the direct shooting method. By comparing all of the plots of the controls and states, one can see that the main difference is the optimal pitch angle trajectory. As mentioned in Chapter 5, since the numerical method used behind direct shooting method for finding the optimal solution is nonlinear programming algorithm, a local optimal solution will be found rather than the global optimal solution. On the other hand, for dynamic programming, a global optimal solution will be found. In this case, the global optimal solution found by DP method is better than the local optimal solution found by the direct shooting method. If one expect to use the direct shooting method to find a global optimal solution, several groups of different initial guesses on the control profiles can be applied and the global optimal solution is chosen as the one with the best performance among them.

However, the direct shooting method has its own advantage over the dynamic programming method. In dynamic programming algorithm, as more controls are involved, more loops need to be calculated. If one wants to get more accuracy by using a smaller discretization step length, the iterations within every loop will increase. Each of the above cases will increase the running time of the DP algorithm. In direct shooting method, since a high efficiency nonlinear programming method is used instead of loops, it usually takes less running time than the dynamic programming algorithm. Remember that only 7 nodes are used in the simulations using the direct shooting method. The performance can be improved by adding more nodes or using smaller integration steps.

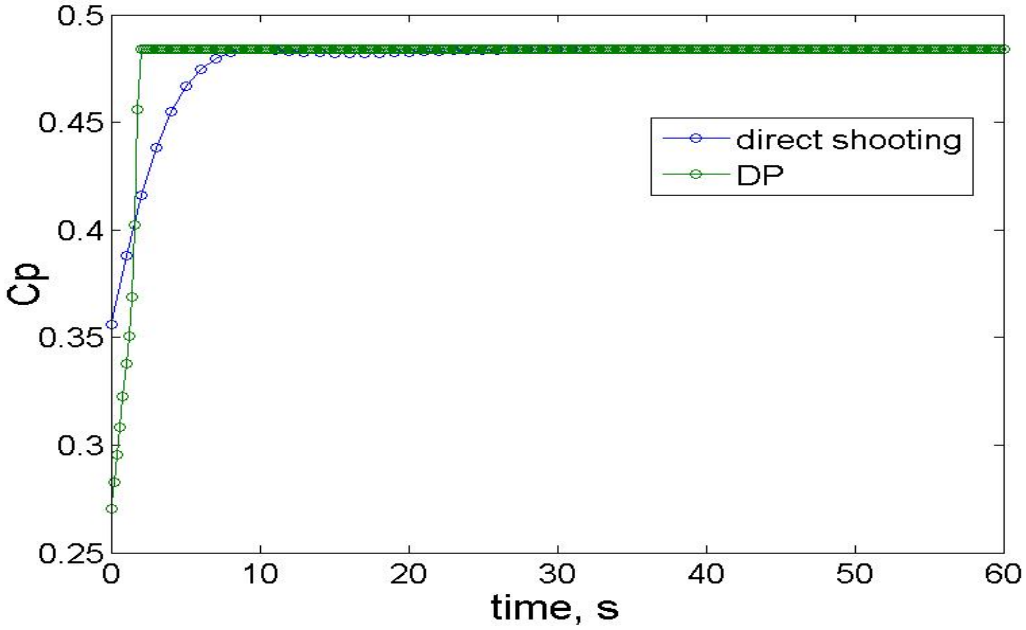


Figure 45: Plot of power coefficient vs. time using the DP and the direct shooting method with a wind speed input of 15 *m/s*.

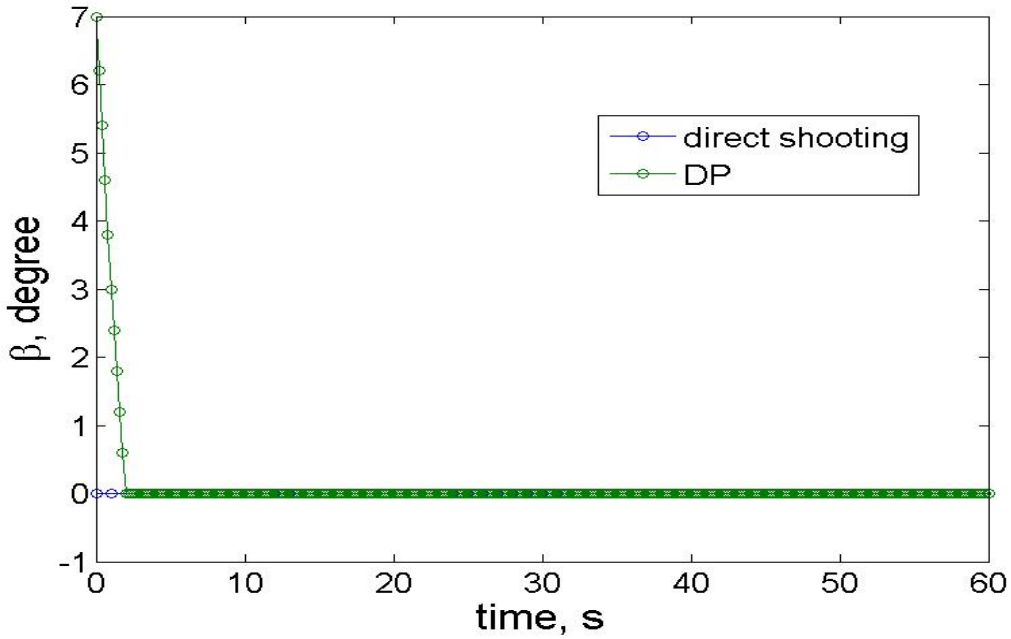


Figure 46: Plot of rotor pitch angle vs. time using the DP and the direct shooting method with a wind speed input of 15 *m/s*.

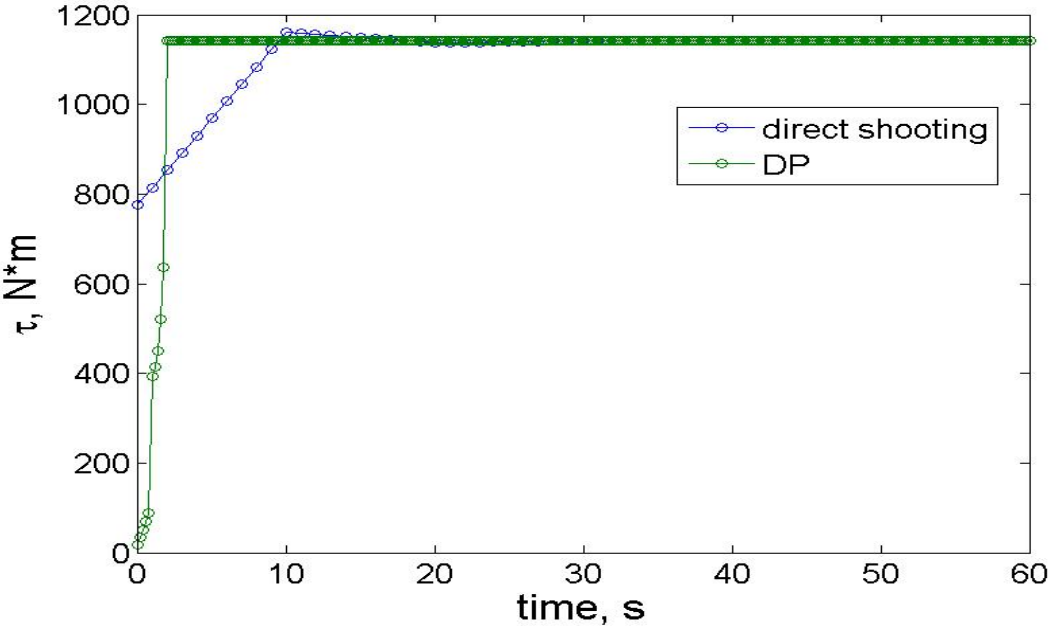


Figure 47: Plot of generator input torque vs. time using the DP and the direct shooting method with a wind speed input of 15 *m/s*.

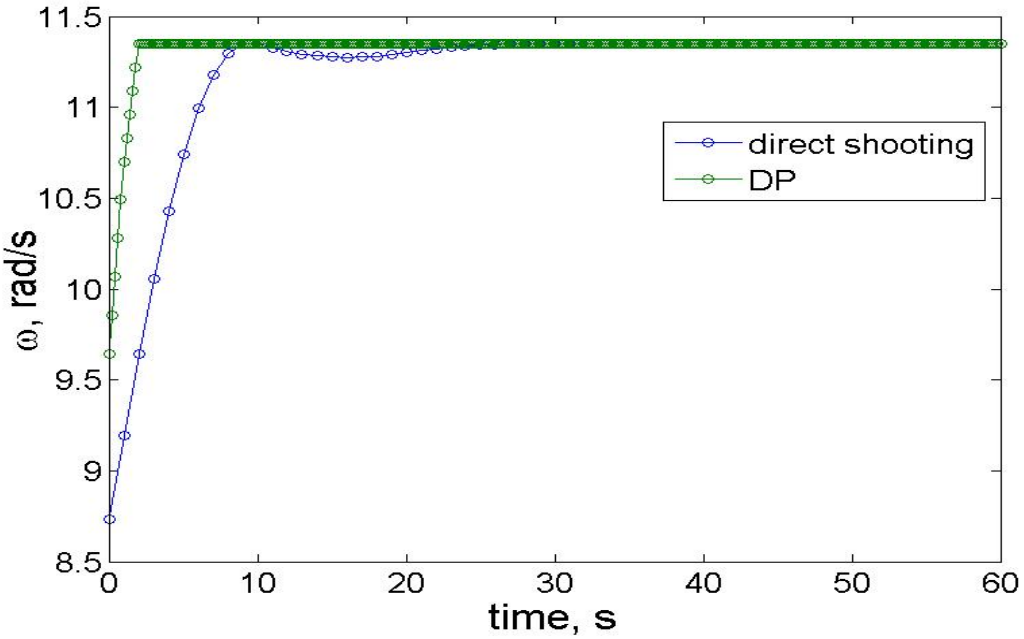


Figure 48: Plot of rotor angular velocity vs. time using the DP and the direct shooting method with a wind speed input of 15 *m/s*.

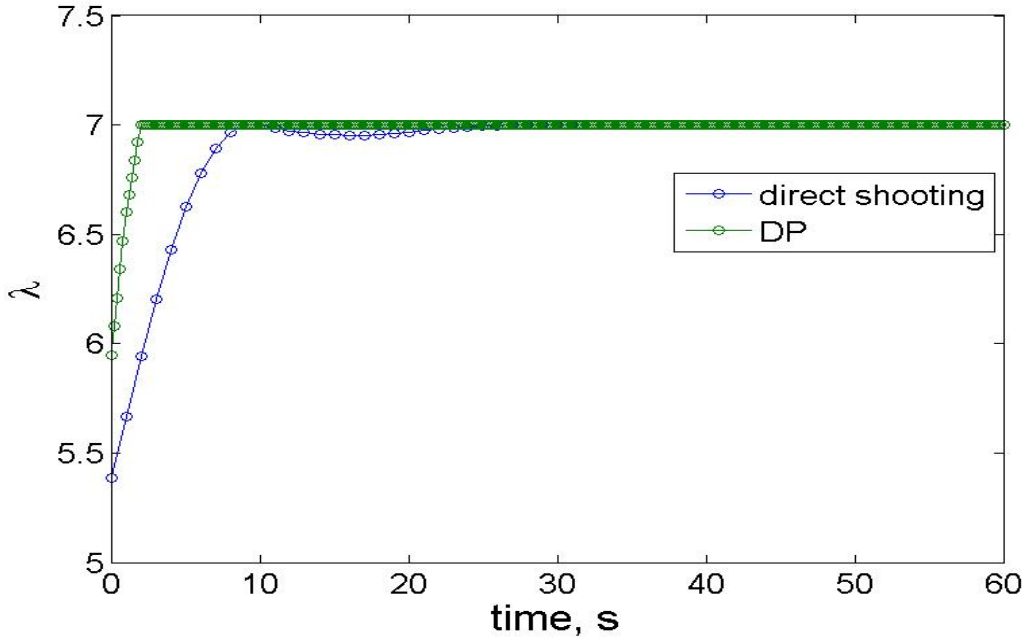


Figure 49: Plot of speed ratio vs. time using the DP and the direct shooting method with a wind speed input of 15 *m/s*.

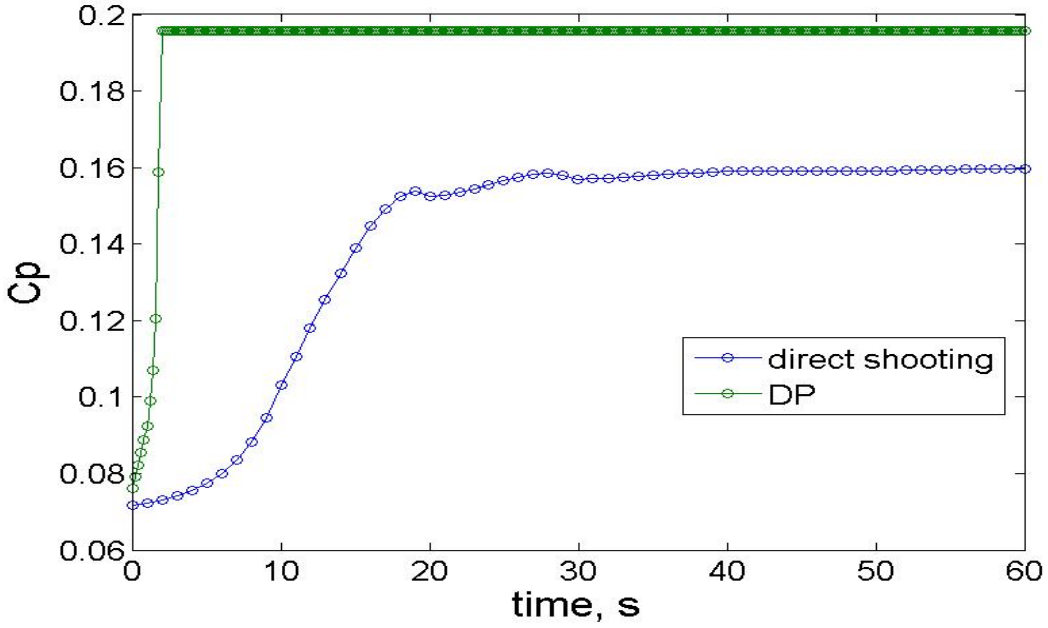


Figure 50: Plot of power coefficient vs. time using the DP and the direct shooting method with a wind speed input of 25 *m/s*.

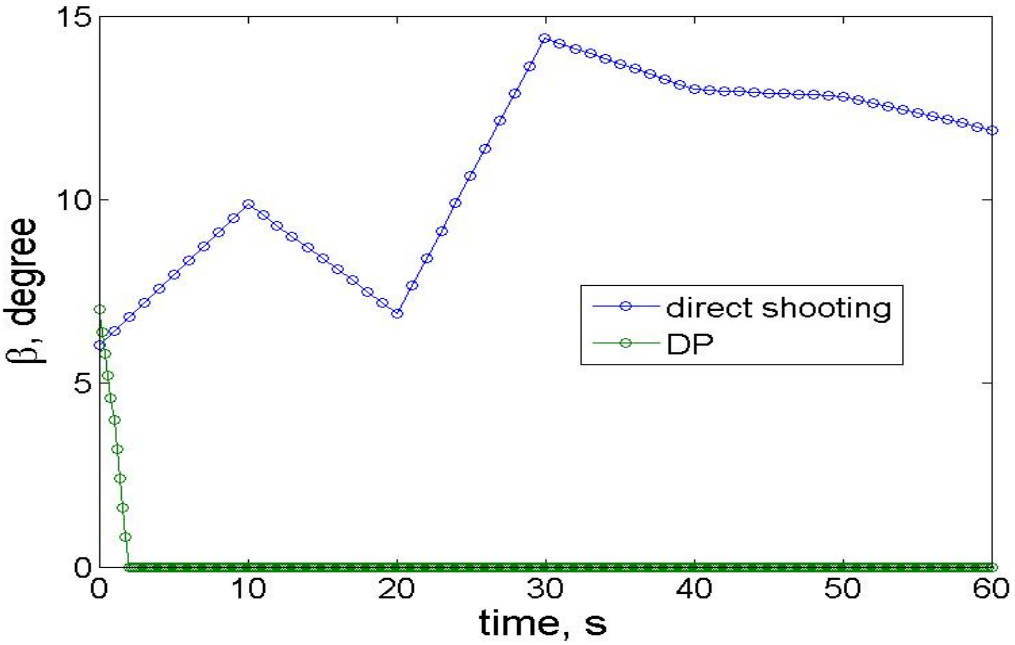


Figure 51: Plot of rotor pitch angle vs. time using the DP and the direct shooting method with a wind speed input of 25 *m/s*.

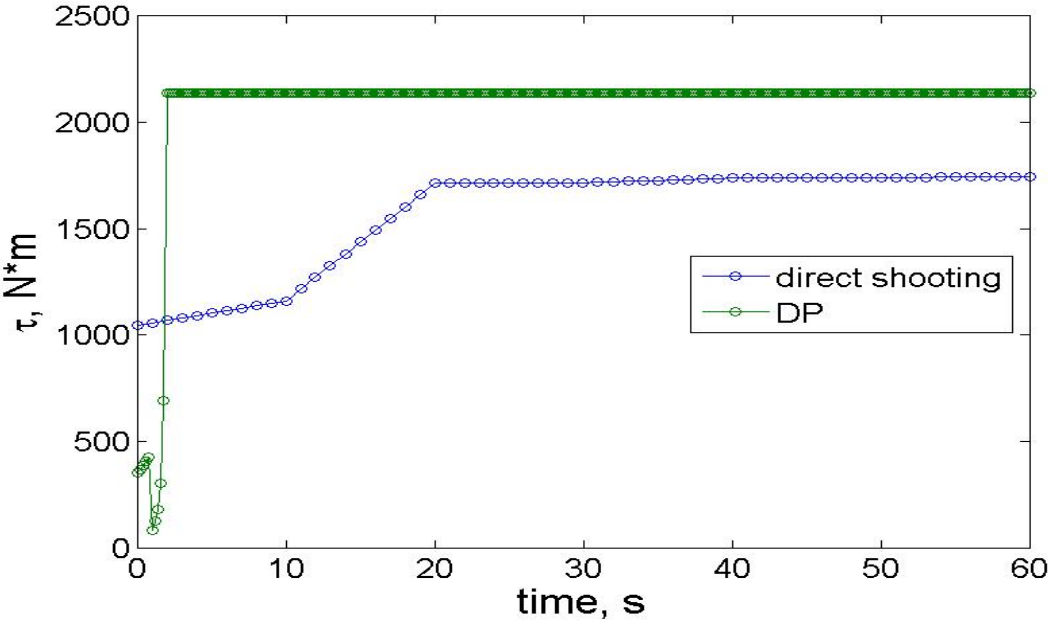


Figure 52: Plot of generator input torque vs. time using the DP and the direct shooting method with a wind speed input of 25 *m/s*.

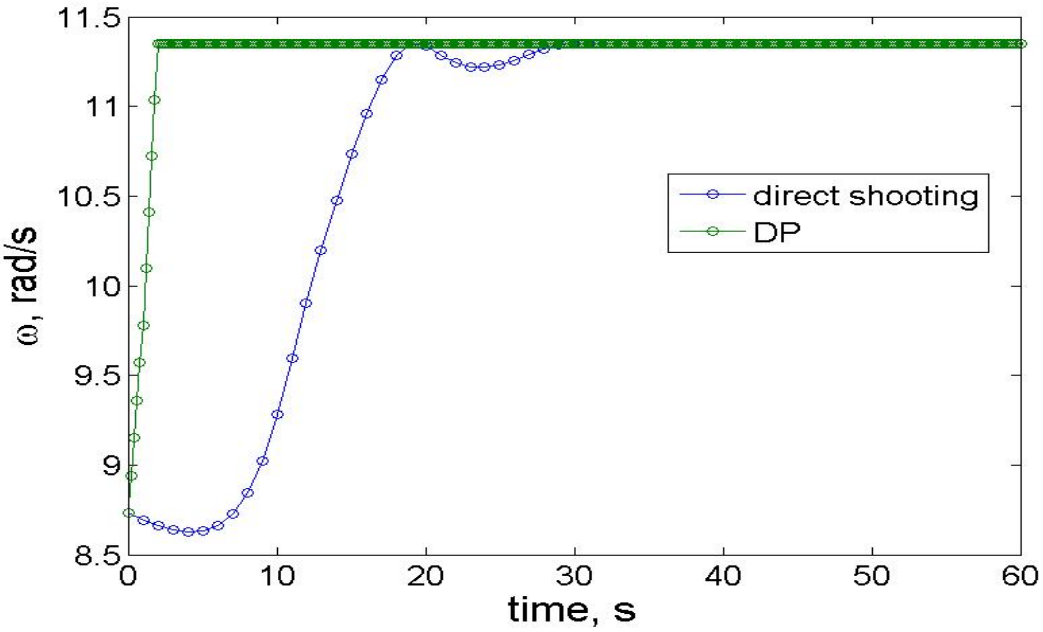


Figure 53: Plot of rotor angular velocity vs. time using the DP and the direct shooting method with a wind speed input of 25 *m/s*.

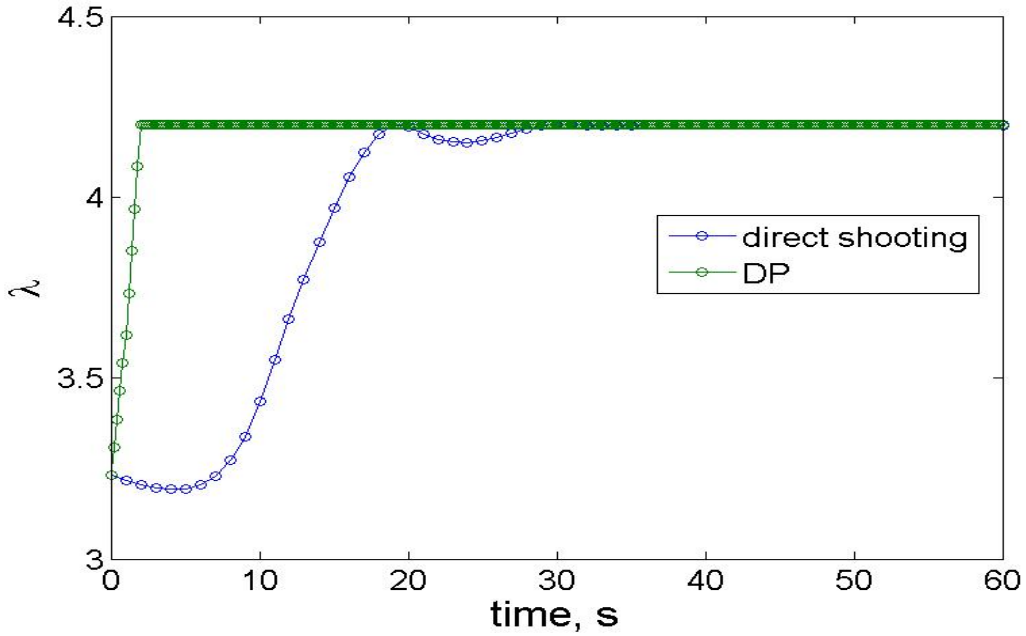


Figure 54: Plot of speed ratio vs. time using the DP and the direct shooting method with a wind speed input of 25 *m/s*.

## COMPARISON BETWEEN MODIFIED FEEDBACK AND DP

As mentioned in Chapter 4, the modified feedback control method with control and states constraints and a predictive controller helping to find the local maximum of the power coefficient curve has a really good performance. The performance is very close to the performance of DP. Figure 55 and 56 show the comparison plots of the power coefficient versus time using DP and modified feedback control method. The first group of simulation lasts for 180 seconds and wind speed inputs are relative low, which are 6, 7 and 8 *m/s* for the 3 intervals. The second group of simulation lasts for 240 seconds and the wind speed inputs are relative high, which are 19, 20, 21 and 22 *m/s*.

Figure 55 shows the simulation result using the first group of wind speed inputs. From the plot, it is seen that as wind speed increases, the steady state value of $C_p$ will also increase. The $C_p$ curve generated by the DP method will reach the steady state much quicker at the beginning of the first interval and a little bit quicker at the beginning of the following intervals than the modified feedback control method.

Figure 56 shows the simulation result using the second group of wind speed inputs. From the plot, it is seen that as wind speed increases, the steady state value of $C_p$ will decrease. However, the same conclusion can be drawn as from Figure 55.

In conclusion, the performance of the modified feedback control is very close to that of the DP method. At the beginning of the first interval, the advantage of the DP method is obvious, while at the beginning of the following intervals, the DP method still has little advantage.

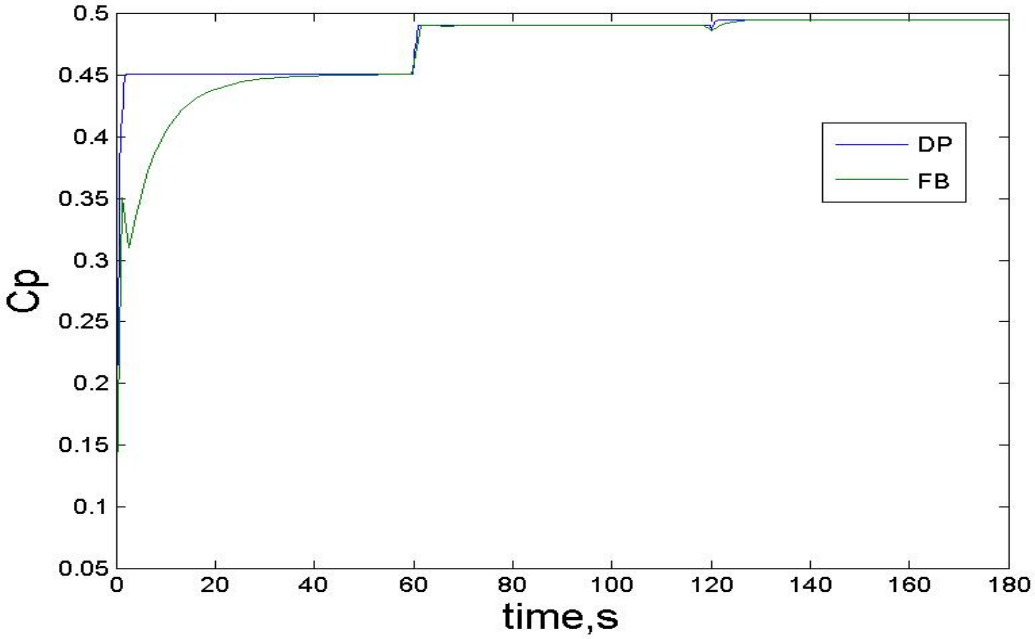


Figure 55: Plot of power coefficient vs. time using the DP and the direct shooting method with the first group of wind speed input.

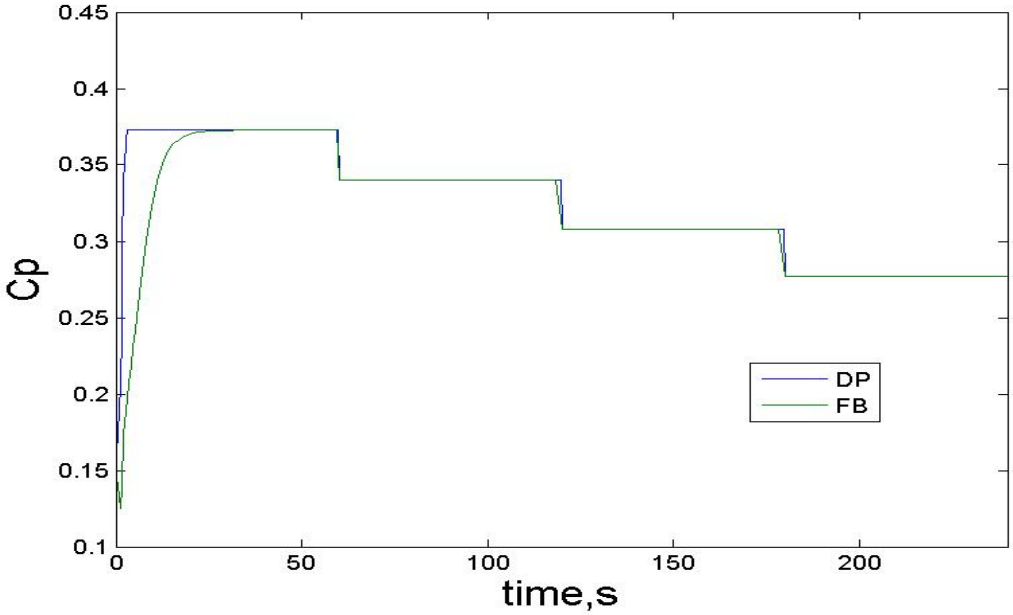


Figure 56: Plot of power coefficient vs. time using the DP and the direct shooting method with the first group of wind speed input.

## CONCLUSION

Three control algorithms, namely the modified feedback control, direct shooting method and dynamic programming approach, were developed and compared in order to maximize the wind turbine aerodynamic coefficient, thus the wind energy capture.

The advantage of the modified feedback control method is that it is very easy to apply. The algorithm is very simple and when the predictive controller is added, the performance is a lot better than the traditional constrained feed back control. The only disadvantage of this method is that the upper limit of the constraint on the generator input torque is highly difficult to apply. When the wind speed input is extremely high, the generator input torque may be too large and out of control.

The direct shooting method has a better performance and the running time is short compared to the DP method. The upper limit on the generator input torque constraint can be well applied. The disadvantage of the direct shooting method is that proper initial guesses on control profiles are necessary for generating a good solution. Sometimes when the initial guesses are not proper, the solution may not be very satisfying and one may need to try groups of different initial guesses and choose the best solution among them.

The DP method has the best performance among all of the 3 methods in quickly reaching the steady state and maximizing the power coefficient value. The constraint on the upper limit of the generator input torque can be well applied. The main disadvantage of the DP method is that many loops and iterations are included, which makes a longer running time compared to the feedback control and the direct shooting method. Although

some iterations or loops can be eliminated that makes the algorithm more efficient, generally the DP method will still take longer running time than other approaches.

# Bibliography

[1] Hurley, Brian. “How Much Wind Energy Is There?”, *Wind Site Evaluation Ltd*, Claverton Group, Retrieved 8 April 2012.

[2] Kahtryn E. Johnson, Lucy Y. Pao, Mark J. Balas, and Lee J. Fingersh, “Control of variable-speed wind turbines, standard and adaptive techniques for maximizing energy capture”, *IEEE Control Systems Magazine*, June 2006, pp. 70-81.

[3] Lucy Y. Pao and Kathryn E. Johnson, “A tutorial on the dynamics and control of wind turbines and wind farms”, *2009 American Control Conference*, Hyatt Regency Riverfront, St. Louis, MO, USA, June 10-12, 2009.

[4] Jason H. Laks, Lucy Y. Pao, and Alan D. Wright, Control of wind turbines: past, present, and furture, *2009 American Control Conference*, Hyatt Regency Riverfront, St. Louis, MO, USA, June 10-12, 2009.

[5] K.E. Johnson, L.J. Fingersh, M.J. Balas and L.Y. Pao, Methods for increasing region 2 power capture on a variable speed HAWT, *the 23rd ASME Wind Energy Symposium*, Reno, Nevada, January 5-8, 2004.

[6] M.M. Hand and M. J. Balas. Systematic controller design methodology for variable – speed wind turbines. *Wind engineering*, 24(3): 169-187, 2000.

[7] J. Yaoqin, Y. Zhongging, and C. Binggang, "A New Maximum Power Point Tracking Control Scheme for Wind Generation", *Proc. IEEE Int. Conf Power Sys. Tech*, pp. 144-148, Oct. 2002.

[8] E. Koutroulis and K. Kalatizakis, "Design of a Maximum Power Tracking System for Wind-Energy Conversion Appications", *IEEE Trans. Ind. Electronics*, 53(2): 386-394, April 2006.

[9] M. J. Balas, Y. J. Lee and L. Kendall, "Disturbance Tracking COntrolTheory with Application to Horizontal Axis Wind Turbines", *Proc. AIAA/ASME Wind Energy Symp*., pp. 95-99, Jan. 1998.

[10] A. D. Wright, "Modern Control Design for Flexible Wind Turbines", *NREL Report* No. TP-500-35816, National Renewable Energy Laboratory, 2004.

[11] Freeman, J. B and Balas, M. J., 1999, An Investigation of Variable Speed Horizontal-Axis Wind Turbines Using Direct Model-Reference Adaptive Control, *Proceeding of the 18th ASME Wind Energy Symposium*, Reno, NV, pp. 66-76.

[12] Song, Y. D., Dhinakaran, B., and Bao, X. Y., 2000, Variable Speed Control of Wind Turbines Using Nonlinear and Adaptive Algorithms*, Journal of Wind Engineering and Industrial Aerodynamics*, 85, pp. 293-308.

[13] Dambrosio, L. and Fortunato, B., 1999, One-Step-Ahead Adaptive Control of a Wind-Driven, Synchronous Generator System, *Energy*, 24, pp. 9-20.

[14] Bossanyi, E. A., 1987, Adaptive Pitch Control for a 250 kW Wind Turbine, *Proceedings of the British Wind Energy Conference*, pp. 85-92.

[15] A. Kumar and K. Stol, "Scheduled Model Predictive Control of a Wind Turbine", *Proc. AIAA/ASME Wind Energy Symp*., Jan. 2009.

[16] http://www.wwindea.org/technology/ch01/en/1_2.html

[17] Stryk, O.V. and Bulirsch, R, Direct and indirect methods for trajectory optimization, *Annals of Operations Research*, v. 37, 1992, pp. 357-373.

[18] David G. Hull, Conversion of optimal control problems into parameter optimization problems, *Journal of Guidance, Control, and Dynamics*, vol.20, No.1, January-Febrary 1997.

[19] Bryson, A.E. and Ho, Y-C, Applied optimal control, *Rev. Printing, Hemisphere*, New York, 1975.

[20] Hestenes, M.R., Calculus of the variations and optimal control theory, *Wiley*, 1966.

[21] Wang, Z, Shen, J.Y., Rowan, B. and Hingwe, P., Optimal seek profile generation with time-varying weightings for hard disk drives, *Microsystem Technology*, vol. 16, 2010, pp.111-115.

[22] Joseph Z. and Ben-Asher, Optimal Control Theory with Aerospace Applications, *AIAA education series*, ISBN 978-1-60086-732-3.

[23] Heier S., Grid integration of wind energy conversion systems, 2nd ed. Hoboken, NJ: *Wiley*; 2006.

[24] NREL, National Renewable Energy Laboratory, http://www.nrel.gov/.

[25] J.F. Manwell and J.G. McGowan, A.L. Rogers, Wind energy explained: theory, design and application, 2nd ed, Chichester, U.K. : *Wiley*, 2009.

[26] http://rredc.nrel.gov/wind/pubs/atlas/tables/1-1T.html